Biogeosciences

Global consequences of afforestation and bioenergy cultivation on ecosystem service indicators

Andreas Krause[1]**, Thomas A. M. Pugh**[1,2,3]**, Anita D. Bayer**[1]**, Jonathan C. Doelman**[4]**, Florian Humpenöder**[5]**, Peter Anthoni**[1]**, Stefan Olin**[6]**, Benjamin L. Bodirsky**[5]**, Alexander Popp**[5]**, Elke Stehfest**[4]**, and Almut Arneth**[1]

[1]Karlsruhe Institute of Technology, Institute of Meteorology and Climate Research – Atmospheric Environmental Research (IMK-IFU), Kreuzeckbahnstr. 19, Garmisch-Partenkirchen, 82467, Germany
[2]School of Geography, Earth & Environmental Science, University of Birmingham, Birmingham, B15 2TT, UK
[3]Birmingham Institute of Forest Research, University of Birmingham, Birmingham, B15 2TT, UK
[4]PBL, Netherlands Environmental Assessment Agency, 2500 GH The Hague, Postbus 30314, the Netherlands
[5]Potsdam Institute for Climate Impact Research (PIK), Telegrafenberg, P.O. Box 60 12 03, Potsdam, 14412, Germany
[6]Department of Physical Geography and Ecosystem Science, Lund University, Lund, 22362, Sweden

Correspondence to: Andreas Krause (andreas.krause@kit.edu)

Abstract. Land management for carbon storage is discussed as being indispensable for climate change mitigation because of its large potential to remove carbon dioxide from the atmosphere, and to avoid further emissions from deforestation. However, the acceptance and feasibility of land-based mitigation projects depends on potential side effects on other important ecosystem functions and their services. Here, we use projections of future land use and land cover for different land-based mitigation options from two land-use models (IMAGE and MAgPIE) and evaluate their effects with a global dynamic vegetation model (LPJ-GUESS). In the land-use models, carbon removal was achieved either via growth of bioenergy crops combined with carbon capture and storage, via avoided deforestation and afforestation, or via a combination of both. We compare these scenarios to a reference scenario without land-based mitigation and analyse the LPJ-GUESS simulations with the aim of assessing synergies and trade-offs across a range of ecosystem service indicators: carbon storage, surface albedo, evapotranspiration, water runoff, crop production, nitrogen loss, and emissions of biogenic volatile organic compounds.

In our mitigation simulations cumulative carbon storage by year 2099 ranged between 55 and 89 GtC. Other ecosystem service indicators were influenced heterogeneously both positively and negatively, with large variability across regions and land-use scenarios. Avoided deforestation and afforestation led to an increase in evapotranspiration and enhanced emissions of biogenic volatile organic compounds, and to a decrease in albedo, runoff, and nitrogen loss. Crop production could also decrease in the afforestation scenarios as a result of reduced crop area, especially for MAgPIE land-use patterns, if assumed increases in crop yields cannot be realized. Bioenergy-based climate change mitigation was projected to affect less area globally than in the forest expansion scenarios, and resulted in less pronounced changes in most ecosystem service indicators than forest-based mitigation, but included a possible decrease in nitrogen loss, crop production, and biogenic volatile organic compounds emissions.

1 Introduction

If the trend in global carbon dioxide (CO_2) emissions observed over the last 2 decades continues, the atmospheric CO_2 concentration is expected to exceed 900 ppm at the end of the 21st century, resulting in a surface temperature increase of several degrees (Friedlingstein et al., 2014; Le Quéré et al., 2015; Peters et al., 2013). However, during the COP21 climate conference in Paris 2015, participating parties agreed to limit global warming to 2 °C or less relative to the pre-industrial era, and by today, 169 countries have rat-

ified the agreement (http://unfccc.int/paris_agreement/items/9485.php, accessed 2 November 2017). The $< 2\,°C$ warming goal requires greenhouse gas (GHG) concentrations to approximately follow or stay below the representative concentration pathway 2.6 (RCP2.6, van Vuuren et al., 2011), which will require serious reductions in CO_2 (and other GHG) emissions across all sectors. Present projections indicate that (1) without substantial net negative CO_2 emissions later this century, the Paris goal will not be achievable (Fuss et al., 2014; Rogelj et al., 2015), and (2) some negative emissions need to be realized in 10–20 years (Anderson and Peters, 2016).

The total carbon dioxide removal (CDR) necessary to achieve the $2\,°C$ target is typically around 100–230 GtC (Rogelj et al., 2015; Smith et al., 2016) depending on the future CO_2 emission pathway and including the need to avoid carbon (C) emissions from further land clearance. Two main strategies of land-based climate change mitigation are commonly discussed for CDR: growth of bioenergy crops in combination with carbon capture and storage (BECCS), and avoided deforestation in combination with afforestation and reforestation (ADAFF) (Humpenöder et al., 2014; van Vuuren et al., 2013; Williamson, 2016). BECCS involves the planting of bioenergy crops or trees, which are burned in power stations or converted to biofuels, and the released CO_2 being captured for long-term underground storage in geological reservoirs. ADAFF utilizes the natural C uptake of forest ecosystems in biomass and soil by maintaining and expanding global forest area.

The total land demand and spatial patterns of these mitigation strategies are highly uncertain due to strong dependencies on underlying assumptions about future environmental and socio-economic changes (Boysen et al., 2017; Popp et al., 2017; Slade et al., 2014). BECCS and ADAFF will likely increase pressure on food-producing agricultural areas and, in the case of BECCS, natural ecosystems. Moreover, similar to other mitigation technologies, the feasibility and effectiveness of BECCS and ADAFF are debated (Keller et al., 2014; Williamson, 2016). For instance, in boreal and many temperate regions tree cover reduces surface albedo, thereby causing local warming (Alkama and Cescatti, 2016). Additionally, reduced CO_2 emissions through forest protection and expansion might be counteracted by cropland expansion in non-forest areas (Popp et al., 2014). BECCS includes substantial economic costs in its CCS component (Smith et al., 2016) and is currently far from being deployable at the commercial scale (Peters et al., 2017; Reiner, 2016). It will also require sufficient safe geologic C storage capacities (Scott et al., 2015). Additionally, the efficiency of BECCS might diminish when C emissions from deforestation (Wiltshire and Davies-Barnard, 2015) or nitrous oxide (N_2O) emissions from bioenergy crops (Crutzen et al., 2008) are considered (with the latter often being accounted for in BECCS scenarios, e.g. Humpenöder et al., 2014).

But even if land-based measures were to be successful with respect to their primary goal of permanently and substantially reducing atmospheric CO_2 levels to mitigate climate change, impacts on ecosystems and societies are likely to be complex (Bennett et al., 2009; Creutzig et al., 2015; Foley et al., 2005; Smith and Torn, 2013; Smith et al., 2013; Viglizzo et al., 2012) and include effects far away from the original land-use (LU) location (DeFries et al., 2004; Rodriguez et al., 2006). The multiplicity of environmental implications caused by large-scale CO_2 removal have so far been largely neglected (Williamson, 2016). The relevance of negative emission technologies, combined with our limited knowledge of their feasibility and risks, encourages the exploration of potential synergies and trade-offs between terrestrial ecosystem services (ESs, defined as benefits that people obtain from ecosystems; MEA, 2005) that are affected in land-based mitigation projects. Such work will facilitate decision-making as to whether the realization of such projects is desirable for society.

In this study, we utilize projections of future LU from one integrated assessment model (IAM, IMAGE) and one LU model (MAgPIE), that are created based on three large-scale land-based mitigation options (BECCS, ADAFF, and a combination of both). Each of these target a CDR of 130 GtC (only CO_2 carbon, omitting other greenhouse gases) by the end of the century, which is approximately equivalent to the cumulative deforestation CO_2 emissions from the late 19th century to today, or around 60 ppm (Le Quéré et al., 2015). We use these spatially explicit LU patterns as input for simulations with the LPJ-GUESS dynamic vegetation model to analyse effects on a variety of ecosystem functions that serve as indicators for important ecosystem services. By using LU patterns from two different LU models we explore some of the uncertainty in indicators of ESs arising from different model assumptions concerning the land demand of land-based mitigation. The main research questions we address in this study are as follows.

1. What are the impacts of land management for carbon uptake on other ecosystem service indicators?

2. Do the effects of land-based climate change mitigation on ecosystem service indicators differ based on the mitigation approach (BECCS, ADAFF, or a combination of both)?

3. If so, can a mitigation approach be identified in which trade-offs between other ecosystem service indicators are less pronounced than in the other approaches?

4. What are the spatial and temporal patterns of the impacts of land-based mitigation on ecosystem service indicators?

This is to our knowledge the first time that global LU scenarios are being used as input to a process-based ecosystem

model to assess changes in ecosystem function and effects on multiple ES indicators.

2 Methods

2.1 LPJ-GUESS

The process-based dynamic global vegetation model (DGVM) LPJ-GUESS simulates vegetation dynamics in response to climate, land-use change (LUC), atmospheric CO_2, and nitrogen (N) input (Olin et al., 2015a; Smith et al., 2014). The model distinguishes between natural, pasture and cropland land-cover types (Lindeskog et al., 2013), all of which include C–N dynamics (Olin et al., 2015a; Smith et al., 2014). Vegetation dynamics in natural land cover are characterized by the establishment, competition, and mortality of 12 plant functional types (PFTs, 10 groups of tree species, C_3 and C_4 grasses) in a number of replicate patches (10 in this study for primary vegetation, 2 for abandoned agricultural areas). Vertical forest structure is accounted for by the use of different age classes for woody PFTs. When forests are cleared for agriculture, 20 % of the woody biomass enters a product pool (turnover time of 25 years), with the rest being oxidized (74 %) or transferred to the litter (6 %). Pastures are populated by C_3 or C_4 grasses which are annually harvested (50 % of above-ground biomass) (Lindeskog et al., 2013). Croplands are represented by prescribed fractions of five crop functional types (CFTs, see Table S1 in the Supplement), which are moderately tilled, fertilized, and harvested (Olin et al., 2015a), and are prescribed to be either irrigated or rain-fed (Lindeskog et al., 2013). Specific bioenergy crops are currently not represented. While LPJ-GUESS does not assume yield increases due to technological progress (in contrast to IMAGE and MAgPIE), climate change adaption is simulated by using a dynamic potential heat unit (PHU) calculation (Lindeskog et al., 2013). The PHU sum needed for the full development of a crop determines its harvesting time. For irrigated crops, water supply is assumed to be available as required to fulfil the plant's water demand. Unmanaged cover grass (C_3 or C_4 type depending on climate) is allowed to grow in croplands between growing seasons.

2.2 The IMAGE and MAgPIE models and the provided land-use scenarios

IMAGE is an IAM model framework that includes several sub-models representing the energy system, agricultural economy, LU, natural vegetation, and climate system (Stehfest et al., 2014). Socio-economic parameters are usually calculated for 26 world regions, and most environmental parameters are modelled on a $0.5° × 0.5°$ grid at annual time steps. LU dynamics are driven by demand for and supply of crops, animal products, and bioenergy. Bioenergy demand to achieve a specific CDR target is determined by the energy system sub-model which uses land availability from the LU

sub-model following a set of sustainability criteria (Hoogwijk et al., 2003). For this study, bioenergy crops are included as fast-growing C_4 grasses (Doelman et al., 2017) as these produce higher yields than woody plants in many locations. The level of agricultural intensification required to free up land for afforestation to achieve a specific CDR target is estimated using a stepwise approach of increasing yields and livestock efficiencies. This implies that reduced crop and pasture areas go with higher yields and livestock efficiencies, thereby allowing the same food production as in the baseline. Afforestation is assumed to occur first in grid cells with high potential for forest growth. IMAGE also represents degraded areas (calibrated so that, together with areas cleared for agriculture, FAO deforestation statistics are met) which can be reforested as part of the afforestation activities (Doelman et al., 2017). Natural vegetation regrowth trajectories as well as crop yields, C, and water dynamics are modelled dynamically by the internally coupled DGVM LPJmL (Bondeau et al., 2007; Stehfest et al., 2014).

MAgPIE is a global multi-regional partial equilibrium model of the agricultural sector (Lotze-Campen et al., 2008; Popp et al., 2014). The model aims to minimize the global costs for agricultural production throughout the 21st century at a 5-year time step (recursive dynamic optimization) and is driven by demand for agricultural commodities and associated costs in 10 world regions. The cost minimization is subject to various spatially explicit biophysical factors such as land and water availability as well as crop yields (provided by LPJmL). Major options to fulfil increasing demand are intensification (yield-increasing technologies), expansion (LUC), and international trade. Demand for CDR enters the model at the global scale, while the spatial distribution of bioenergy production or afforestation is derived endogenously in the model (involving economic and biophysical factors). Bioenergy demand is fulfilled chiefly through the growth and harvest of grassy energy crops; woody bioenergy in this study is grown only on less than 1 % of the area used for bioenergy. Actual bioenergy yields are derived from potential LPJmL yields (using information about observed LU intensity and agricultural area for initialization) but can exceed LPJmL yields over time due to technological progress (Humpenöder et al., 2014). Afforestation is assumed to occur as managed regrowth of natural vegetation according to parameterized s-shaped growth curves towards a maximum potential natural vegetation C density as provided by LPJmL, with soil C increasing linearly towards its potential maximum within 20 years (Humpenöder et al., 2014). For simplicity, we refer to both IMAGE and MAgPIE as LU models (LUMs) in the following.

As input to our study we use the baseline projections (without land-based mitigation) from IMAGE and MAgPIE, and three land-based mitigation scenarios, each calculated by both LUMs, based on the assumption of a cumulative CDR target of 130 GtC by the year 2100. In the "BECCS" scenario this is achieved via bioenergy plant cultivation and sub-

sequent CCS, the "ADAFF" scenario involves maintaining and expanding global forest area, and in "BECCS-ADAFF" the CDR demand is fulfilled in equal parts via both options. While the CDR target in ADAFF is achieved via terrestrial C uptake (CDR = Δ vegetation C + Δ soil C + Δ product pool), in BECCS it is fulfilled solely via CCS (CDR = cumulative CCS) and thus did not account for changes in vegetation and soil C. The baseline scenario ("BASE") involves no land-based mitigation but LUC takes place in response to, among other factors, increasing food demand, dependent on population and GDP growth. LUC was provided by the LUMs as net land-cover transitions. Wood harvest was not accounted for in the data provided by the LUMs. All scenarios were developed with RCP2.6 climate produced by the IPSL-CM5A-LR general circulation model (GCM), bias corrected to the 1960–1999 historical period (Hempel et al., 2013). The LU scenarios were created using harmonized assumptions about climate change, atmospheric composition, and socio-economic development and thus did not include C cycle feedbacks. As it seems currently unlikely that the RCP2.6 pathway can be achieved without any land-based mitigation (Fuss et al., 2014), the BASE scenario should rather be regarded as a diagnostic scenario to isolate the LU effects induced by the mitigation scenarios from other factors. CO_2 fertilization effects on plant growth were simulated in the LUMs' crop growth and vegetation models. Both LUMs harmonized their cropland and pasture LU patterns to the spatially explicit HYDE 3.1 dataset (Klein Goldewijk et al., 2011) in the year 1995 (MAgPIE) or 2005 (IMAGE), with small deviations in the area of the land-cover classes occurring due to different land masks and calibration routines. The simulation period was 1970–2100 in IMAGE and 1995–2100 in MAgPIE. Socio-economic developments as input to the LUMs were based on the Shared Socioeconomic Pathway 2 (SSP2, "Middle of the Road") (O'Neill et al., 2014; Popp et al., 2017). We only used spatially explicit LU and land management (irrigation and synthetic plus organic N fertilizer) patterns from the LUMs as input to the LPJ-GUESS simulations; other variables also available from the LUMs (e.g. C stocks or crop production) were calculated with LPJ-GUESS. Details about the conversion of IMAGE and MAgPIE-LU data to LPJ-GUESS input data can be found in Supplement Sect. S1.

Even though MAgPIE and IMAGE derive crop yields and C densities from the same DGVM (LPJmL; Bondeau et al., 2007), the land demand to meet the same CDR target is larger in IMAGE than in MAgPIE. This reflects different model approaches: while in IMAGE bioenergy cultivation can only be established in unproductive regions not needed for food production, in MAgPIE there is a competition for land between food production and land-based mitigation. Concerning afforestation, managed regrowth (according to prescribed growth curves) is assumed in MAgPIE while in IMAGE natural regrowth dynamically calculated within LPJmL is implemented. Consequently, bioenergy production in MAgPIE is located in regions with mostly higher yields compared to

IMAGE, and forest regrowth occurs at a faster rate, resulting in less LUC and mitigation actions starting later in the MAgPIE scenarios (Fig. 1, Table S2). In the BASE scenario, the area under natural vegetation decreases throughout the future for both IMAGE and MAgPIE (Fig. 1, Table S2), but more so for IMAGE due to the representation of degraded forests (which are treated as grassland in IMAGE; see Supplement Sect. S1). Substantial regional differences between both LUMs exist by the end of the century in the BASE scenario (Fig. 2a). Avoided deforestation and afforestation in the ADAFF scenarios is chiefly located in the tropics (Fig. 2b) and afforestation typically takes place on pastures or degraded forests in IMAGE but on croplands in MAgPIE (Table S2). Bioenergy production area in BECCS is increased mainly at the expense of natural vegetation in IMAGE but taken also from existing agricultural land in MAgPIE. Total cropland area increases in the scenario combining both strategies (BECCS-ADAFF) compared to BASE for IMAGE but decreases for MAgPIE BECCS-ADAFF (Fig. 1). IMAGE uses a slightly larger grid list than MAgPIE and accounts for the water fraction of a grid cell; but as the impacts on land-based mitigation in LPJ-GUESS turned out to be small (< 2 GtC over the simulation period) we only included grid cells in our simulations for which LU data were provided by both LUMs (assuming 100 % land cover) to facilitate comparison of the results.

2.3 Simulations setup

The LPJ-GUESS simulations were forced by daily atmospheric climate variables (surface temperature, precipitation, shortwave radiation) extracted from bias-corrected simulated IPSL-CM5A-LR RCP2.6 climate (1950–2099) from the first phase of ISI-MIP project (Warszawski et al., 2014). For the historical period we randomly chose years from the period 1950–1959 to generate climate data for the years 1901–1949. A repeating climate cycle from the 1901–1930 period was used for the model's spin-up. The global average surface temperature increase in IPSL-CM5A-LR is 1.3 °C (1.6 °C on land) by the end of the century (2070–2099) compared to present-day (1980–2009) for RCP2.6. This value is in the middle of an ensemble of a wider range of GCM models used in ISI-MIP (Warszawski et al., 2014). Historical (1901–2005) and future (RCP2.6, 2006–2099) atmospheric CO_2 mixing ratios were taken from Meinshausen et al. (2011). The year 1901 value (296 ppmv) was used for the spin-up. Future atmospheric CO_2 mixing ratio peaks at 443 ppmv in year 2052 and drops to ∼ 424 ppmv by the end of the century (Meinshausen et al., 2011). Gridded N deposition rates were available as decadal monthly averages for the historical and future (RCP2.6) period (Lamarque et al., 2010, 2011). N deposition for year 1901 was used for the spin-up. Spatially explicit LU patterns and N fertilization were adopted from IMAGE and MAgPIE (see also Supplement Sect. S1). We used the year 1901 land-cover map for the spin-up, thereby
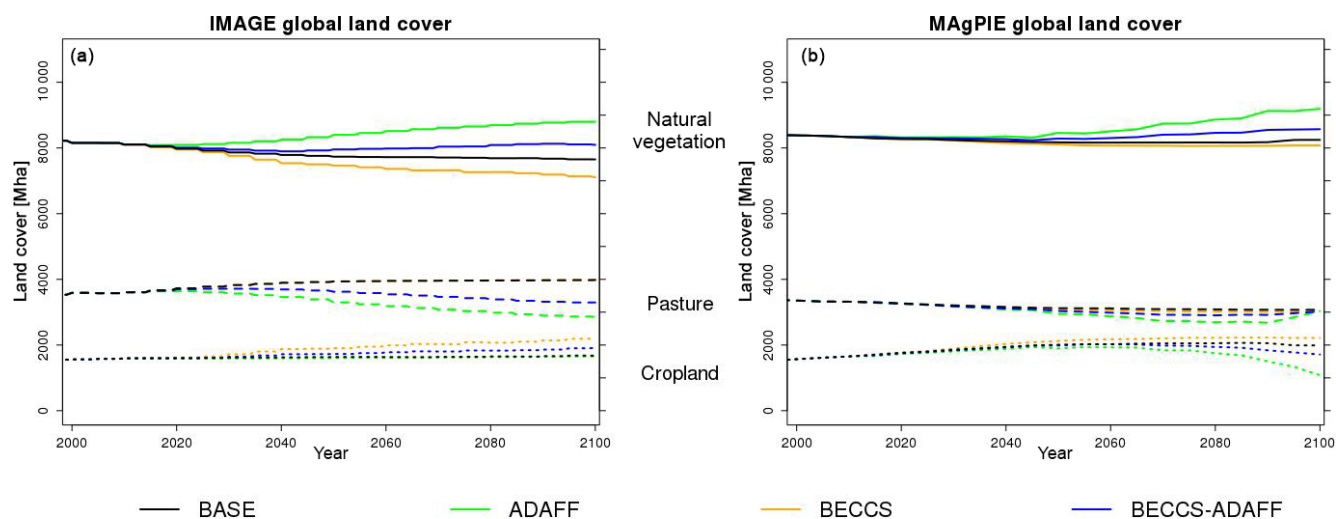
Figure 1. Time series (2000–2100) of area under natural vegetation (including afforested area), pasture (including degraded forest area for IMAGE), and cropland (including bioenergy production area) for the different scenarios, for IMAGE **(a)** and MAgPIE **(b)**.

omitting LUC occurring before the 20th century as we assumed legacy effects from pre-1901 LUC on the future C cycle to be small.

2.4 Analysed ecosystem service indicators

We analysed the implications of future LU patterns for the following ES indicators: C storage (as an indicator for global climate change mitigation), surface albedo and evapotranspiration (indicators for regional climate effects in response to land-cover change), annual runoff (indicator for water availability), peak monthly runoff (indicator for flood protection), crop production (excluding cotton, forage crops, and pasture harvest; indicator for food production), N loss (in LPJ-GUESS currently not differentiated into dissolved N vs. N lost to the atmosphere; indicator for water or air quality, or GHG losses), and emissions of the most common biogenic volatile organic compounds (BVOCs) – isoprene and monoterpenes (indicator for air quality). With the exception of C storage and crop production these variables were not available from the LUMs. Most variables are direct outputs from LPJ-GUESS simulations. Calculations for ES indicators not taken directly from model outputs (C storage via CCS, crop production scaled to EarthStat, albedo) or different from the standard model setup (BVOCs) are provided in the Supplement Sects. S2–S5.

The analysed ES indicators can serve as proxies for several ESs linked to human well-being. Table 1 gives a qualitative overview of how these ES indicators and corresponding ESs are interlinked. We do not aim to value and rank individual ES indicators and thus do not assess here how relative changes could be differently prioritized in decision-making for land management. While this is certainly too simple of a generalization for fully assessing the implications of such

scenarios, ranking or prioritizing individual ES indicators is a substantial challenge, which is beyond the scope of this study. A given relative change can be more crucial for some indicators than for others, and their importance can also vary across regions and parties concerned. ESs will be influenced by changes in climate, atmospheric chemistry, and LU even in the absence of land management for C mitigation. To separate these non-mitigation effects from those effects associated with a mitigation approach, we compared changes in ES indicators in the BASE simulations over the 21st century to the changes that occur when a mitigation approach is implemented. Land-based mitigation may thus potentially enhance or degrade ESs to human societies.

3 Results

In the following, the expressions "LPJG$_{IMAGE}$" and "LPJG$_{MAgPIE}$" refer to results from LPJ-GUESS simulations driven by LU patterns from IMAGE and MAgPIE, plus climate, CO_2, and N deposition from RCP2.6. At some points we refer to output directly taken from the IMAGE and MAgPIE scenarios, in which case this is explicitly stated ("in the original results/directly from the LUMs /the LUMs report").

3.1 Carbon storage

Total global C pools simulated with LPJ-GUESS are generally lower for LPJG$_{IMAGE}$ than for LPJG$_{MAgPIE}$ for all scenarios (Table 2, Fig. S1a). This difference is mainly a result of the representation of degraded forests as grasslands in IMAGE-LU patterns (see Table S2), while MAgPIE does not include degraded forests. Moreover, some temperate croplands that are specified in the MAgPIE-LU patterns to grow fodder are represented in LPJ-GUESS by rain-fed or irri-
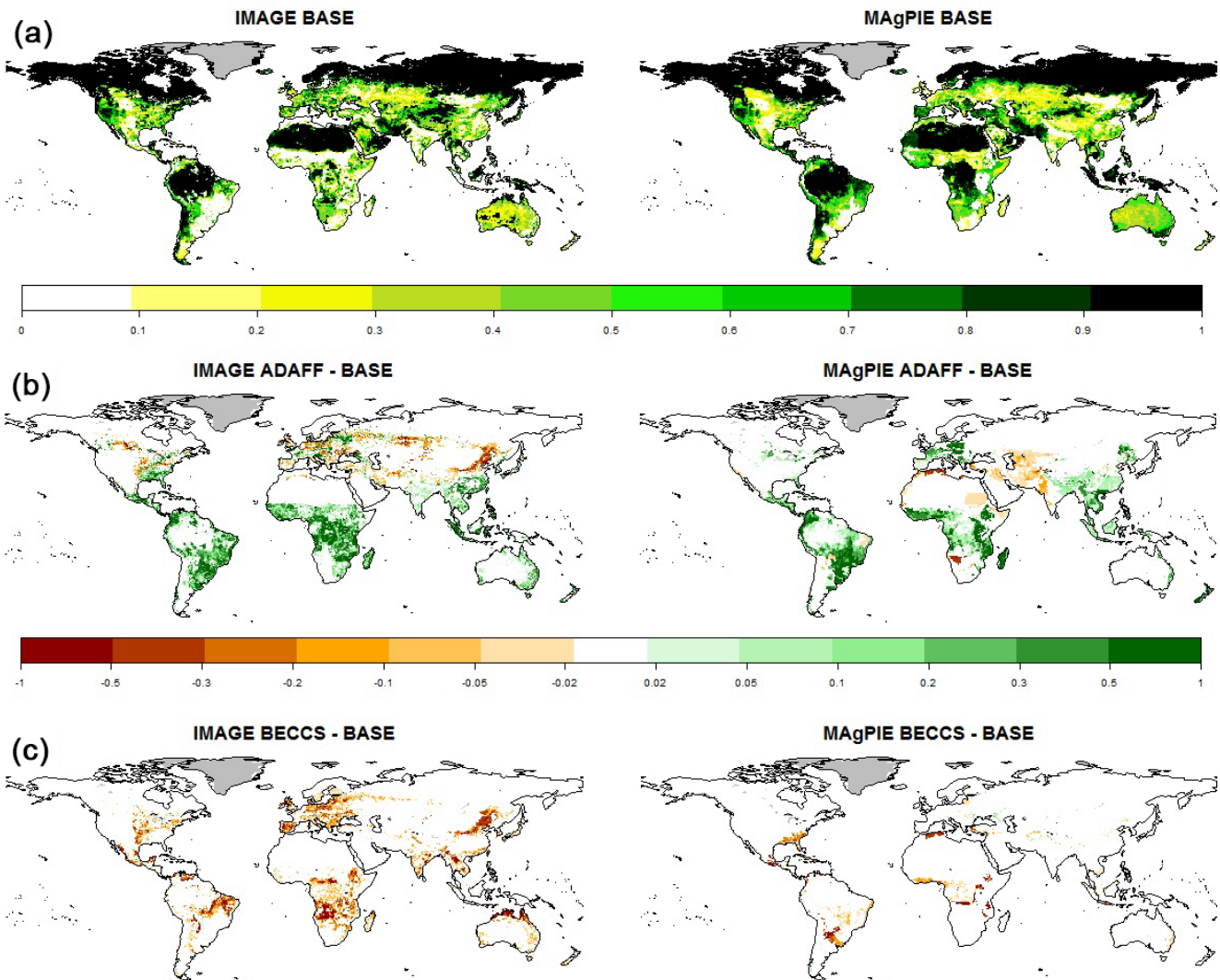
Figure 2. (a) Fraction of grid cell under natural vegetation (including afforested area but not degraded forests) by the end of the century (2090–2099) in the BASE scenario for IMAGE (left) and MAgPIE (right). **(b)** Difference in the natural vegetation fraction between the ADAFF and the BASE scenario by the end of the century (2090–2099). **(c)** Same as panel **(b)** but between the BECCS and the BASE scenario.

gated, harvested grass. This crop type increases soil C relative to cereal crops because the larger below-ground / above-ground biomass ratio results in less C being removed during harvest and thus more C input to the soil. C sequestration is calculated by LPJ-GUESS for both BASE simulations within the 21st century, resulting in total C pools of 1995 (LPJG$_{\mathrm{IMAGE}}$) and 2047 (LPJG$_{\mathrm{MAgPIE}}$) GtC by 2090–2099 (Table 2). The combined effects of LU, changing climate, N deposition, and atmospheric CO_2 levels thus enhance total C pools by 1.7 and 3.2 % (33 and 64 Gt) between the beginning and the end of the century (Fig. 3a).

As expected from the overall scenario objective, total, vegetation, and soil C pools are higher in the ADAFF simulations relative to the respective BASE at the end of the century

(Table 2, Fig. S1a–c). The additional C uptake for ADAFF is larger for LPJG$_{\mathrm{IMAGE}}$ (3.6 % or 72 GtC in year 2090–2099, 76 GtC in year 2099) than for LPJG$_{\mathrm{MAgPIE}}$ (2.4 % or 49 GtC in year 2090–2099, 55 GtC in year 2099, Fig. 3b). This reflects the larger afforestation area and earlier afforestation activities in IMAGE (Figs. 1, 2b). The largest changes in total C are found in tropical regions, especially in Africa (+15 and +9 %, Fig. 4b) and/or tropical forests (+13 and +8 %, Fig. S2b), mostly due to increases in vegetation C.

The BECCS scenario focusing on bioenergy crops and CCS as a climate change mitigation strategy removes slightly less C from the atmosphere than ADAFF for LPJG$_{\mathrm{IMAGE}}$ but removes more C for LPJG$_{\mathrm{MAgPIE}}$ (Table 2, Fig. 3c). Interestingly, LPJG$_{\mathrm{IMAGE}}$ ADAFF accumulates more C than

Table 1. Linking ecosystem functions to ecosystem services (ESs). An increase in an ecosystem function can be interpreted positive (+), negative (−), zero (0), or either positive or negative (+/−), depending on the background conditions or perspective. Effects can be small (+ or −) or large (++ or −−). Regional effects are shown without brackets and global effects, where relevant, in brackets. Indirect effects that are more directly represented by another ecosystem function considered here are not shown. The table is based on evidence from the literature in cases where the link is not directly clear (see footnotes).

Ecosystem function	ES – climate change mitigation	ES – water availability	ES – flood protection	ES – water quality	ES – air quality	ES – food production
C storage ↑	++ (++)					
Surface albedo ↑	++ (+)[a]					
Evapotranspiration ↑	++ (+/−)[b]					
Annual runoff ↑		++	−	0/+[c]		
Peak monthly runoff ↑		0/+[d]	−−	0/−[e]		0/−[f]
Crop production ↑						++ (++)
N loss ↑	+/− (+/−)[g]			−−[g]	− (−)[g]	
BVOC emissions ↑	+/− (+/−)[h]				0/ −− (0/−)[i]	

[a] The global effects of LU-driven albedo changes seem to be small (e.g. de Noblet-Ducoudre et al., 2012).
[b] Local surface cooling as heat is needed to evaporate water. On larger scales, the effect could be either a warming due to increases in atmospheric water vapour (Boucher et al., 2004) or a cooling due to increased planetary albedo resulting from more cloudiness (Bala et al., 2007; Ban-Weiss et al., 2011).
[c] High flows imply more volume for dilution, prevent algae growth, and maintain oxygen levels (Whitehead et al., 2009).
[d] Effect of peak monthly runoff on water availability is dependent on seasonal rainfall distribution and regional water storage capacity. Annual runoff is the clearer indicator.
[e] Soil erosion and associated remobilization of metals is enhanced during flood events (Whitehead et al., 2009).
[f] Due to flood damage in croplands (Posthumus et al., 2009).
[g] LPJ-GUESS at present calculates total N loss and does not differentiate between leaching and gaseous loss. Thus, we indicate several effects that would arise from N emitted as N_2O (a greenhouse gas), as NO_X or NH_3 (affecting air quality and aerosol formation), or as dissolved N. The net effect of N loss on climate has been estimated to be a small cooling (Erisman et al., 2011), but uncertainties are large.
[h] The net impact of BVOC emissions is very uncertain. On the global scale, increased BVOC emissions might result in a warming (Unger, 2014).
[i] BVOCs often increase ozone and aerosol formation, primarily locally (Rosenkranz et al., 2015), with principally opposite warming and cooling effects (Unger, 2014).
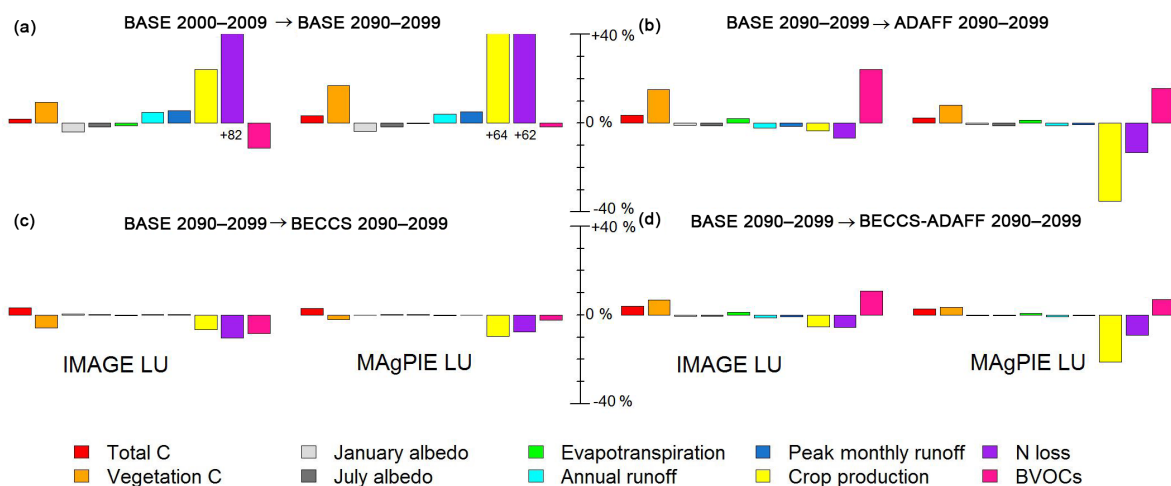
Figure 3. Global relative changes in analysed ecosystem functions simulated by LPJ-GUESS for different LU scenarios from IMAGE and MAgPIE. Changes are capped at ±40 % for clarity reasons, and values exceeding 40 % are written below the bar. **(a)** Changes in the BASE simulation from 2000–2009 to 2090–2099. **(b)** Changes from BASE to ADAFF by the 2090-2099 period. **(c)** Same as panel **(b)** but from BASE to BECCS. **(d)** Same as panel **(b)** but from BASE to BECCS-ADAFF.

LPJG$_{IMAGE}$ BECCS within the first half of the century, while BECCS catches up during the second half of the century (Fig. S1a); this acceleration of the BECCS sink is related to a steady increase in bioenergy area throughout the century. The additional total C storage achieved by the period 2090–2099 (compared to BASE 2090–2099) is 66 GtC (74 GtC in year 2099) for LPJG$_{IMAGE}$ and 61 GtC (69 GtC in year 2099) for LPJG$_{MAgPIE}$. Within these totals, cumulative C storage via CCS (harvested C from bioenergy crops) is 100 and 74 GtC by the end of the century (Table 2), but total C uptake is less than cumulative CCS as LPJ-GUESS simulates a loss of vegetation and soil C from expanded agricultural land. C stor-

Table 2. Global net-total values ± standard deviations (over 10 years) of all analysed ecosystem functions as simulated by LPJ-GUESS for all scenarios and different time periods and for LPJG$_{IMAGE}$ (top) and LPJG$_{MAgPIE}$ (bottom). Total C is the sum of vegetation C, soil C, product C (wood removed during deforestation but not immediately oxidized), and cumulative CCS.

Ecosystem function	BASE		ADAFF	BECCS-ADAFF	BECCS
	2000–2009		2090–2099		
Vegetation C	380 ± 1	415 ± 2	478 ± 4	444 ± 3	391 ± 2
(GtC)	393 ± 2	459 ± 2	496 ± 5	476 ± 3	450 ± 2
Soil and litter C	1575 ± 1	1578 ± 1	1588 ± 1	1580 ± 1	1567 ± 1
(GtC)	1585 ± 1	1587 ± 1	1599 ± 2	1592 ± 2	1583 ± 1
Product C	5.7 ± 0.4	1.5 ± 0.1	0.4 ± 0.0	1.0 ± 0.1	2.4 ± 0.2
(GtC)	4.6 ± 0.2	0.3 ± 0.0	0.4 ± 0.0	0.3 ± 0.0	0.6 ± 0.1
Cumulative CCS	–	–	–	52.1 ± 3.4	100.0 ± 6.6
(GtC)	–	–	–	34.7 ± 2.5	73.5 ± 5.6
Total C	1961 ± 2	1995 ± 3	2067 ± 5	2077 ± 7	2060 ± 7
(GtC)	1983 ± 2	2047 ± 3	2096 ± 7	2103 ± 7	2108 ± 8
January albedo	0.250 ± 0.004	0.240 ± 0.002	0.237 ± 0.002	0.238 ± 0.002	0.241 ± 0.002
	0.249 ± 0.004	0.240 ± 0.002	0.238 ± 0.002	0.240 ± 0.002	0.240 ± 0.002
July albedo	0.182 ± 0.001	0.179 ± 0.001	0.177 ± 0.001	0.178 ± 0.001	0.180 ± 0.001
	0.182 ± 0.001	0.179 ± 0.001	0.177 ± 0.001	0.178 ± 0.001	0.179 ± 0.001
Evapotranspiration	58.6 ± 0.7	57.9 ± 1.2	59.1 ± 1.2	58.6 ± 1.2	57.7 ± 1.2
(1000 km^3 yr^{-1}*)	58.9 ± 0.7	58.8 ± 1.2	59.5 ± 1.2	59.3 ± 1.2	58.9 ± 1.2
Annual runoff	52.5 ± 3.1	55.1 ± 2.8	53.9 ± 2.8	54.4 ± 2.8	55.3 ± 2.8
(1000 km^3 yr^{-1})	52.2 ± 3.1	54.3 ± 2.8	53.7 ± 2.8	53.9 ± 2.8	54.2 ± 2.8
Peak monthly runoff	17.9 ± 1.0	18.9 ± 1.2	18.7 ± 1.2	18.8 ± 1.2	19.0 ± 1.2
(1000 km^3 month^{-1})	17.9 ± 1.0	18.8 ± 1.2	18.6 ± 1.2	18.7 ± 1.2	18.8 ± 1.2
Crop production	28.9 ± 0.5	35.9 ± 0.5	34.7 ± 0.5	34.0 ± 0.5	33.5 ± 0.5
(Ecal)	27.5 ± 0.9	45.2 ± 0.4	29.3 ± 2.0	35.5 ± 0.7	40.8 ± 0.5
N loss	60.3 ± 7.1	109.7 ± 13.2	102.3 ± 12.5	103.6 ± 12.3	98.4 ± 11.5
(TgN yr^{-1})	73.3 ± 6.8	119.0 ± 8.0	103.2 ± 8.4	108.1 ± 7.9	110.0 ± 7.0
Isoprene emissions	477 ± 8	419 ± 9	529 ± 11	469 ± 10	382 ± 8
(TgC yr^{-1})	503 ± 9	495 ± 10	578 ± 13	532 ± 11	483 ± 10
Monoterpene emissions	40.7 ± 0.6	38.9 ± 0.9	40.2 ± 1.0	39.4 ± 0.9	38.2 ± 0.9
(TgC yr^{-1})	41.9 ± 0.7	40.5 ± 0.9	41.6 ± 1.0	40.9 ± 0.9	40.4 ± 0.9

* 1000 km^3 are equal to 1 Eg of water.

age in the combined bioenergy–avoided deforestation and afforestation case (BECCS–ADAFF) mostly lies between the BECCS and the ADAFF case but for LPJG$_{IMAGE}$ exceeds both ADAFF and BECCS by the end of the century (Table 2, Figs. 3d, S1a, S3).

3.2 Albedo

Globally averaged January albedo under present-day conditions is significantly higher (~ 0.25) than July albedo (~ 0.18) due to the extensive northern hemispheric snow cover in January. Both values decrease throughout the 21st century in the BASE simulations, but more so for January (-4.1 and -3.7 % for LPJG$_{IMAGE}$ and LPJG$_{MAgPIE}$, respectively) than for July (-1.7 and -1.8 %) as a result of northward vegetation shifts and reductions in snow cover (Table 2, Figs. 3a, S1d–e). Regionally, for both months and both LUMs, the greatest reductions occur in high latitudes (Fig. 4a).

An increase in forested area as in the ADAFF scenario results in further albedo reductions that are – at least for July albedo – comparable in magnitude to the changes in BASE throughout the century (Table 2, Fig. 3b). Only small increases compared to BASE occur in the BECCS simulations
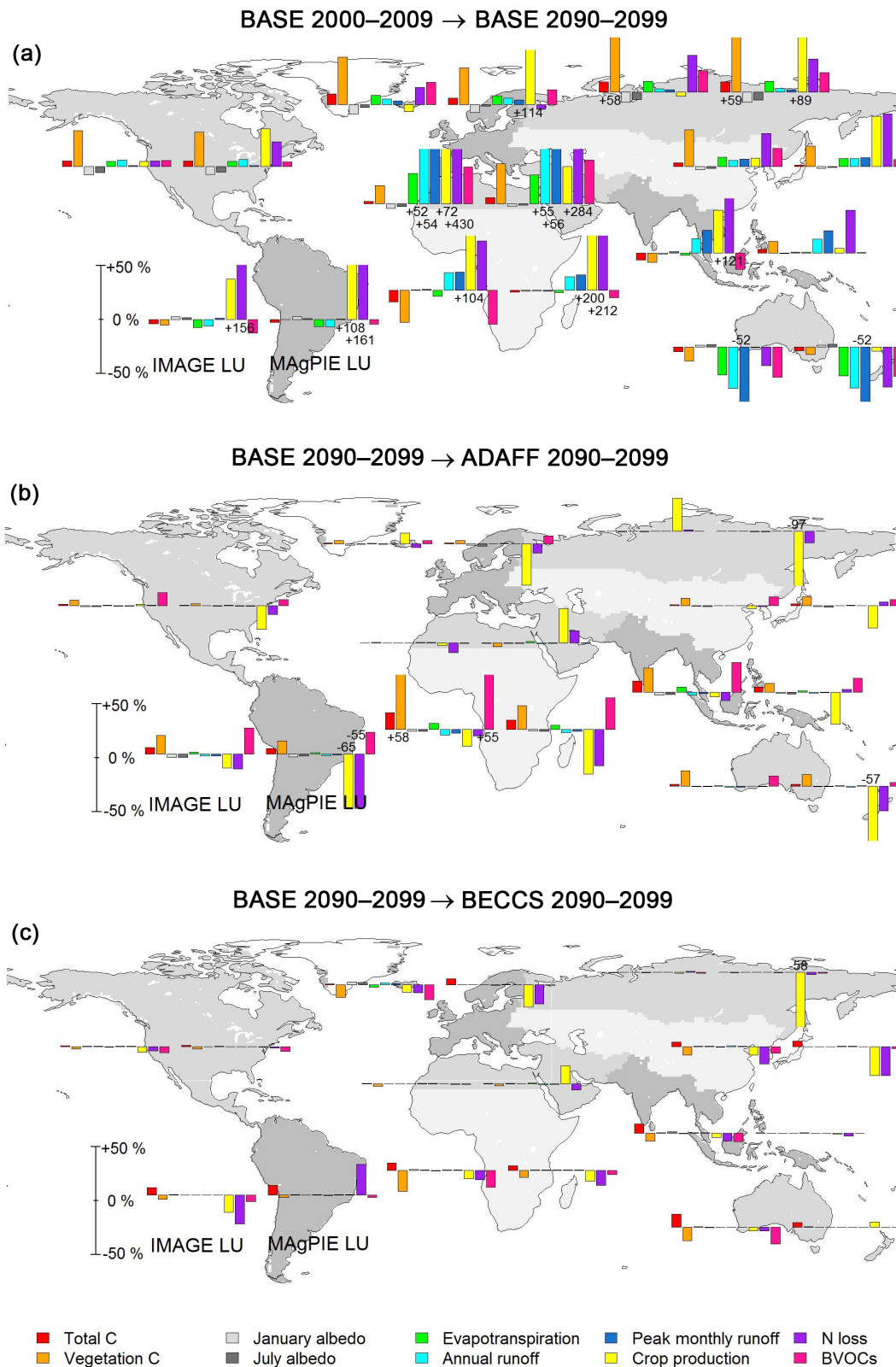
Figure 4. Regional relative changes in analysed ecosystem functions as simulated by LPJ-GUESS for IMAGE-LU (left) and MAgPIE-LU (right). Changes are capped at ±50 % for clarity reasons, values exceeding ±50 % are written upon or below the bar. Regions are aggregated Global Fire Emissions Database regions (Giglio et al., 2010) and are North America, South America, Europe, Middle East, Africa, North Asia, Central Asia, South Asia, and Oceania. **(a)** Changes in the BASE simulation from 2000–2009 to 2090–2099. **(b)** Changes from BASE to ADAFF by the 2090–2099 period. **(c)** Same as panel **(b)** but from BASE to BECCS.

(Fig. 3c) as the land demand for bioenergy crop cultivation is relatively small. BECCS-ADAFF results in a decrease in January and July albedo for both LUMs.

3.3 Evapotranspiration

Global evapotranspiration in the BASE simulations decreases much more for LPJG$_{IMAGE}$ (-1.2%) than for LPJG$_{MAgPIE}$ (0.1%; Table 2, Figs. 3a, S1f) due to different deforestation rates. There is large spatial variability with evapotranspiration decreasing in some regions but increasing in others (Fig. 4a), mainly driven by shifting rainfall patterns (not shown).

As expected from the generally high evapotranspiration rates of forests, end-of-century evapotranspiration in ADAFF is 2.1 and 1.3 % higher than in BASE for LPJG$_{IMAGE}$ and LPJG$_{MAgPIE}$, respectively (Fig. 3b), with the largest increase occurring in Africa (Fig. 4b). BECCS results in a change of -0.4 and $+0.2\%$ for LPJG$_{IMAGE}$ and LPJG$_{MAgPIE}$, respectively, and BECCS-ADAFF in an increase of 1.3 and 0.8 % compared to BASE.

3.4 Runoff

In the BASE simulations, global annual runoff increases by 4.9 and 4.1 % by the end of the century for LPJG$_{IMAGE}$ and LPJG$_{MAgPIE}$, respectively, with a slightly larger increase of 5.2 and 5.0 % in peak monthly runoff (Table 2, Fig. 3a). This increase is mainly driven by precipitation changes, but forest loss and increased water use efficiency simulated under elevated CO$_2$ levels also play a role. Similar to evapotranspiration, spatial patterns are heterogeneous, with generally larger changes in annual runoff than in peak monthly runoff in high latitudes and reverse patterns in parts of the (sub-) tropics (Figs. 4a, S2a).

Changes in runoff in the mitigation simulations are opposite to evapotranspiration changes (Figs. 3b–d, 4b–c), and the effects of land-based mitigation on annual runoff are often larger than on peak monthly runoff. ADAFF reduces annual runoff by 2.2 and 1.1 % (LPJG$_{IMAGE}$ and LPJG$_{MAgPIE}$) and peak monthly runoff by 1.3 and 0.7 %, while BECCS increases annual runoff by 0.3 and 0.2 % and peak monthly runoff by 0.2 and 0.0 %.

3.5 Crop production

Globally, total crop production simulated by LPJ-GUESS averages ~ 29 and $27\,\mathrm{Ecal\,yr^{-1}}$ over the years 2000–2009 and increases by 24 and 64 % to 36 and 45 Ecal yr^{-1} by the end of the century for the LPJG$_{IMAGE}$ and LPJG$_{MAgPIE}$ BASE simulations, respectively (Table 2, Fig. S1i) (for comparison, the increase is 78 and 96 % in the original IMAGE and MAgPIE results, respectively). The large differences in crop production increase between LPJG$_{IMAGE}$ and LPJG$_{MAgPIE}$ can be explained by variations in management and crop types (e.g. whether the LUMs assume C$_3$ or C$_4$

crops to be grown in certain regions), and the area and location of managed land, which differs considerably by the end of the century, especially in Africa (Fig. 2a). Sensitivity simulations in which N fertilizer rates, cropland area, atmospheric CO$_2$ mixing ratio, or the dynamic PHU calculation (i.e. adaption to climate change via selecting suitable crop varieties, see Sect. 2.1) were fixed at year 2009 levels indicate that around 62 and 39 % (LPJG$_{IMAGE}$ and LPJG$_{MAgPIE}$, respectively) of the crop production increase in the BASE simulations can be attributed to increases in N fertilizer rates, 22 and 74 % to cropland expansion, 26 and 10 % to increased atmospheric CO$_2$ levels, and 9 and 4 % to dynamic PHU calculation (Fig. S4a). The numbers do not add up to 100 % due to non-linear effects, interdependencies between variables (crop area/fertilization), and additional influences we did not analyse (e.g. climate, N deposition, crop types, and irrigation).

Crop production calculated with LPJ-GUESS is reduced in all mitigation simulations compared to BASE, by contrast to a set requirement in the LUMs to retain annual production at similar levels to BASE: in the LUMs this is achieved through further technology increases (for example through improved management, inputs, pest control, and better crop varieties) compared to BASE. The decline simulated in LPJ-GUESS, which is larger for LPJG$_{MAgPIE}$ than for LPJG$_{IMAGE}$, especially for ADAFF (LPJG$_{IMAGE}$ -3% for the 2090–2099 period compared to 2090–2099 BASE; LPJG$_{MAgPIE}$ -35%), occurs because LPJ-GUESS captures only yield increases achieved through higher N input, which only covers a part of the additional technological yield increase assumed by the LUMs for the mitigation scenarios (and which therefore allows for shrinking production area, see Table S2).

3.6 Nitrogen loss

Global N loss in the BASE simulations increases strongly over the 21st century by 82 % for LPJG$_{IMAGE}$ and 62 % for LPJG$_{MAgPIE}$ (Fig. 3a). Most of the increase is caused by fertilization but increasing N deposition contributes as well ($+19\%$ over the century). N loss is higher for LPJG$_{MAgPIE}$ than for LPJG$_{IMAGE}$ at the beginning and end of the 21st century, but higher for LPJG$_{IMAGE}$ around mid-century (Table 2, Fig. S1j). As total fertilizer application is higher for LPJG$_{MAgPIE}$ throughout the entire century, these differences can be explained by spatial heterogeneity (e.g. in India, where fertilization has a large impact on N loss, fertilizer rates are generally higher for LPJG$_{IMAGE}$ than for LPJG$_{MAgPIE}$). Increases in N losses correspond roughly to increases in N application, and to crop production increases in the original LUMs. This indicates that crops in LPJ-GUESS approach N saturation, and cannot use the additional N for higher yields, and thus that N application rates, while consistent with LUM yield levels, are too high for LPJ-GUESS yields. Sensitivity simulations indicate that most of the N loss increase between 2000–2009 and 2090–2099 is in-

duced by increased fertilizer application and cropland expansions, while increasing atmospheric CO_2 and dynamic PHU calculation reduce N loss (Fig. S4b).

N loss in ADAFF decreases by 6.7 % for LPJG$_{IMAGE}$ and 13.2 % for LPJG$_{MAgPIE}$ compared to BASE 2090–2099 (Fig. 3b), but with large variability across regions (Fig. 4b). The decrease can be attributed to lower global fertilizer amounts in ADAFF than in BASE for both LUMs, as forests are not fertilized. In the BECCS simulations the decrease is larger for LPJG$_{IMAGE}$ (−10.3 %) than for LPJG$_{MAgPIE}$ (−7.6 %), including substantial regional variations, especially in South America (Fig. 4c). The fertilization of bioenergy crops (for which low fertilizer rates are assumed in the LUMs) adds N to the system; however, crop N uptake and subsequent removal during harvest are also enhanced, resulting in a net N removal in LPJ-GUESS (and thus less N available to leave the system via leaching or in gaseous form). N loss reductions in BECCS-ADAFF lie between ADAFF and BECCS for LPJG$_{MAgPIE}$ (−9.2 %) but are smallest amongst all mitigation simulations for LPJG$_{IMAGE}$ (−5.5 %).

3.7 BVOCs

Changes in BVOC emissions are dominated by isoprene emissions, which are, by weight, an order of magnitude higher than those of monoterpenes (Table 2, Fig. S1k–l). In the BASE simulations, total BVOC emissions from 2000–2009 to 2090–2099 decrease by 11 % for LPJG$_{IMAGE}$ but only by 2 % for LPJG$_{MAgPIE}$ (Fig. 3a). Spatially, BVOC emissions generally increase in high latitudes but decrease in the tropics (Fig. 4a), corresponding to northward forest shifts and deforestation or forest degradation concentrated in low latitudes (not shown). The tropics dominate the overall response due to much higher typical emission rates.

As expected from the generally high emission potential of woody vegetation (compared with herbaceous), BVOC emissions increase in the ADAFF simulations (24 and 16 % for LPJG$_{IMAGE}$ and LPJG$_{MAgPIE}$, respectively). Following the spatial change in forest cover, the increase mainly occurs in the tropics (Fig. 4b). In the BECCS simulations, BVOC emissions decrease by 8 % for LPJG$_{IMAGE}$ and by 2 % for LPJG$_{MAgPIE}$ (Fig. 3c) due to the low emissions of grassy bioenergy crops (corn in LPJ-GUESS). BECCS-ADAFF results in 11 and 7 % higher emissions for LPJG$_{IMAGE}$ and LPJG$_{MAgPIE}$, respectively (Fig. 3d).

4 Discussion

4.1 Modelling uncertainties under present-day and future climate

The ES indicators analysed in this study are subject to uncertainties arising from knowledge gaps, simplified modelling assumptions, and the need to use parameterizations suited for global simulations. LPJ-GUESS has been extensively evaluated against present-day C fluxes and stocks, both for natural and agricultural systems, at site scale and against global estimates (e.g. Fleischer et al., 2015; Piao et al., 2013; Pugh et al., 2015; Smith et al., 2014). The use of forcing climate data from only one climate model can be a major source of uncertainty as shown by the large variability in future terrestrial C stocks introduced by different climate change realizations even for the same emissions pathway (Ahlström et al., 2012). As we use the low-emission scenario RCP2.6 here, we expect this effect to be relatively small. The albedo calculation in this study was not used previously, but patterns simulated by LPJ-GUESS under present-day conditions (Fig. S5) broadly agree with Fig. 3 in Boisier et al. (2013). Evapotranspiration and runoff in LPJ were evaluated by Gerten et al. (2004). Global total runoff calculated in this study for the 1961–1990 period is 26 % higher than their results. Simulation biases against global estimates and observations from large river basins in the Gerten study were mainly attributed to uncertainties in climate input data and to human activities such as LUC (which is now accounted for) and human water withdrawal. Spatial runoff patterns as simulated by the current LPJ-GUESS version (Fig. S6.) seem to reveal some improvements compared to the biases reported in Gerten et al. (2004) in mid- and high latitudes, but the model still overestimates runoff in parts of the tropics. With respect to crop production, simulated crop yields in LPJ-GUESS are constrained by N and water limitation, but not by local management decisions, crop varieties or breeds, diseases, and weeds (Lindeskog et al., 2013; Olin et al., 2015b), and future improvement in plant breeding are ignored. While we accounted for the additional restrictions by scaling simulated present-day yields to observations, applying the unscaled LPJ-GUESS yield changes into the future might create substantial underestimation of future yields and crop production, as the only yield-augmenting factor for a given crop type in LPJ-GUESS is increased N input. Global N-leaching rates are highly uncertain but the annual rate simulated with LPJ-GUESS (if all N losses are assumed to be via leaching) is within the range of published studies (Olin et al., 2015a). Future modelled N leaching may also be affected by ignoring improvements in plant breeds, as the current representation of crops may not be able to absorb the N input computed in the LUMs for improved varieties and management. For BVOCs, global datasets for evaluation are not available (Arneth et al., 2007; Schurgers et al., 2009). Spatial emission patterns are in good agreement with other simulations (Hantson et al., 2017).

While LPJ-GUESS has thus been evaluated as comprehensively as possible, a further next step for multi-process evaluation would be adopting a formalized benchmarking system that also allows model performance to be scored (Kelley et al., 2013). Likewise, large uncertainties reside in the actual LUMs, which differ to a large degree in their estimates of main land-cover classes for the present day (Alexander et al., 2017; Prestele et al., 2016), and for which evaluation against

observations has been identified as a challenge (van Vliet et al., 2016).

4.2 Climate regulation via biogeochemical and biophysical effects

Our LPJG$_{IMAGE}$ simulations are slightly more effective than the LPJG$_{MAgPIE}$ simulations in terms of simulated C uptake, but all simulations diverge from the CDR target initially implemented in the LUMs (see Sect. 4.7). Land-based mitigation might also impact the emissions of other GHGs (e.g. N$_2$O; see Table 1), but future fertilizer application rates and emissions from bioenergy crops are highly uncertain (Davidson and Kanter, 2014). While N$_2$O contributes to global warming, the net effect of reactive N might be a cooling when accounting for short-lived pollutants and interactions with the C cycle (Erisman et al., 2011). In our LPJ-GUESS simulations, reductions in N losses suggest a decrease in gaseous N emissions for both ADAFF and BECCS; however, no quantifications are possible as LPJ-GUESS does not yet differentiate between different forms of N losses.

Climate effects of well-mixed GHG are global, whereas biophysical effects are primarily felt on the local scale (Alkama and Cescatti, 2016). Surface albedo in regions with seasonal snow cover is expected to decrease significantly for afforestation scenarios (Bala et al., 2007; Bathiany et al., 2010; Betts, 2000; Davies-Barnard et al., 2014), thereby opposing the biogeochemical cooling effect. Effects of enhanced forest cover are less pronounced in lower latitudes (Li et al., 2015) and for BECCS scenarios (Smith et al., 2016). A modelling study by Hallgren et al. (2013) found that while albedo effects and C emissions from deforestation for biofuel production might balance on the global scale, biophysical effects can be large locally. In our BECCS simulations, albedo changes are relatively small. However, we find noticeable albedo reductions in ADAFF despite the fact that for both LUMs afforestation was concentrated in snow-free regions where satellites rarely observe albedo differences between forests and open land exceeding 0.05 (Li et al., 2015).

High evapotranspiration rates, often observed in forests, cool the local surface. In tropical regions, this cooling effect exceeds the warming effect from lower albedo (Alkama and Cescatti, 2016; Li et al., 2015). Current anthropogenic land-cover changes have been estimated to reduce terrestrial evapotranspiration by ∼ 5 % (Sterling et al., 2013). In our simulations, impacts of land-based mitigation on global evapotranspiration range from −0.4 % (LPJG$_{IMAGE}$ BECCS) to +2.1 % (LPJG$_{IMAGE}$ ADAFF). On the regional scale this can translate to absolute changes of more than 100 mm yr^{-1} in some tropical areas (e.g. central Africa). While these changes seem relatively small compared to the mean differences between forests and non-forests reported by Li et al. (2015) (141 mm yr^{-1} 20–50° N, 238 mm yr^{-1} 20–50° S, 428 mm yr^{-1} 20° S–20° N), our results still suggest that reducing emissions from deforestation and forest degradation

(REDD) activities would not only help mitigate global climate change via avoided C losses but could provide additional local cooling, serving as a "payback" for tropical countries. The simulated evaporative water loss due to ADAFF at the end of the century (∼ 1200 km^3 yr^{-1} for LPJG$_{IMAGE}$ and 750 km^3 yr^{-1} for LPJG$_{MAgPIE}$ for a C sequestration rate of ∼ 0.8 and 1.4 GtC yr^{-1}, respectively) is higher than estimated by Smith et al. (2016) (370 km^3 yr^{-1} for a C sequestration rate of ∼ 1.1 GtC yr^{-1}). Furthermore, Smith et al. (2016) assumed that dedicated rain-fed bioenergy crops consume more water than the replaced vegetation (with additional water required for CCS), while in our simulations bioenergy crops had little impact on evapotranspiration as they were represented as corn. LU-driven changes in evapotranspiration rates can also modify the amount of atmospheric water vapour and cloud cover, with consequences for direct radiative forcing, planetary albedo, and precipitation (e.g. Sampaio et al., 2007, see also Table 1); however, such interactions cannot be captured by our model setup.

BVOCs influence climate via their influence on tropospheric ozone, methane, and secondary organic aerosol formation (Arneth et al., 2010; Scott et al., 2014), which depend strongly on local conditions such as levels of nitrogen oxides (NO$_X$) or background aerosol (Carslaw et al., 2010; Rosenkranz et al., 2015). BVOC emissions also impact climate directly by reducing terrestrial C stocks, but the magnitude is small (< 0.5 %) compared to total GPP. While enhanced leaf-level BVOC emissions are driven by warmer temperatures, uncertainties arise from additional CO$_2$ effects (which suppress leaf emissions). On the canopy scale, isoprene emissions generally decrease for deforestation scenarios (Hantson et al., 2017) but increase for woody biofuel plantations, which tend to use high-emission tree species (Rosenkranz et al., 2015). In our simulations, we find increases in BVOC emissions for ADAFF but not so for BECCS as bioenergy crops were grown as low-emission corn. The high spatial and temporal variability of the BVOC emissions, complications of atmospheric transport, and gaps in our knowledge of the reactions involved make it difficult to judge whether an increase in BVOC emissions results in a warming or cooling. The global effect (assuming present-day air pollution in 1850 and excluding aerosol–cloud interactions) of historic (1850s–2000s) reductions in BVOC emissions (20–25 %) due to deforestation has been estimated to be a cooling of −0.11 ± 0.17 W m^{-2} (Unger, 2014). Accordingly, the substantial increase in BVOC emissions in our ADAFF simulations (16 and 24 %) might induce a warming of similar magnitude.

4.3 Water availability

Forests generally reduce local river flow compared to grass- and croplands. Based on 26 catchment datasets including 504 observations worldwide, Farley et al. (2005) reported an average decrease of 44 and 31 % in annual stream flow caused

by woody plantations replacing grasslands and shrublands, respectively, with large variability across different plantation ages. Simulations by Sterling et al. (2013) suggest that historic land-cover changes were responsible for a 7 % increase in total runoff. The reduction in global annual runoff due to ADAFF (1200 and 600 km^3 yr^{-1} compared to BASE 2090–2099) corresponds to around 16–32 % of human runoff withdrawal (Oki and Kanae, 2006), which could be seen as a potential risk to freshwater supply. Regional changes range from −5.2 to +0.4 % across all scenarios, but in many cases impacts on irrigation (the largest consumer of freshwater) potential in fact might be small: modelling work suggests that renewable water supply will exceed the irrigation demand in most regions by the end of the century for RCP8.5 (Elliott et al., 2014). However, Elliott et al. (2014) also found that regions with the largest potential for yield increases from increased irrigation are also the regions most likely to suffer from water limitations. Patterns will be different in an RCP2.6 world as CO_2 fertilization significantly reduced global irrigation demand (8–15 % on presently irrigated area) in the Elliott et al. crop models and climate impacts are expected to be less severe in RCP2.6.

In uncoupled simulations, such as those carried out here, atmospheric feedbacks related to higher evapotranspiration cannot be captured. At regional or continental scale, there is evidence that afforestation might actually increase runoff as the larger evapotranspiration rates enhance precipitation (Ellison et al., 2012). However, based on regional climate modelling, Jackson et al. (2005) concluded that atmospheric feedbacks were not likely to offset water losses in temperate regions where the additional atmospheric moisture cannot be lifted high enough to form clouds.

Changing runoff affects water supply but can also contribute to changes in flood risks. Bradshaw et al. (2007), using a multi-model approach and data from 56 developing countries, calculated a 4–28 % increase in flood frequency and a 4–8 % increase in flood duration for a hypothetical reduction of 10 % natural forest cover, while van Dijk et al. (2009), for example, questioned forest potential to reduce large-scale flooding and argued that the frequency of reported floods can be mainly explained by population density. Ferreira and Ghimire (2012) extended the original Bradshaw sample to all countries (129) that reported at least one large flood between 1990 and 2009 and included socio-economic factors in their analyses. They did not find a statistically significant correlation between forest cover and reported floods. In our simulations, peak monthly runoff is generally reduced for ADAFF; however, given maximum regional changes of −3.6 % (Africa, LPJG$_{IMAGE}$ ADAFF) and presuming that floods are largely controlled by other factors than forest cover, we expect LU effects on flooding to be limited.

4.4 Food production

Increasing food production in a sustainable way to feed a growing population is a major challenge of the modern world (Tilman et al., 2002). Population and income growth (in SSP2 population peaks in 2070 at 9.4 billion people, and per capita GDP continues to increase until 2100; Dellink et al., 2017; Samir and Lutz, 2017) are projected to be accompanied by an increased need of total calories and shifts in diets (Popp et al., 2017). For SSP2, economic modelling suggests that global food crop demand will increase by 50–97 % between 2005 and 2050 (Valin et al., 2014). In the present study, the corresponding increase reported directly from the LUMs is 38 % for IMAGE and 52 % for MAgPIE in 2050 (78 and 96 % in year 2100). In our LPJ-GUESS BASE simulations we find crop production increases of 22 and 45 % (LPJG$_{IMAGE}$ and LPJG$_{MAgPIE}$, respectively) by 2050 and 24 and 64 % by the end of the century (corresponding to a per capita increase for MAgPIE but a decrease for IMAGE). However, the production increase is significantly reduced in the mitigation simulations, especially for LPJG$_{MAgPIE}$ ADAFF, due to production shifts and the abandonment of croplands for reforestation. Similar results have been reported by Reilly et al. (2012) who found that afforestation substantially increases prices for agricultural products, while the cultivation of biofuels has little impact on agricultural prices due to benefits of avoided environmental damage offsetting higher mitigation costs. Crop yields in LPJ-GUESS are a function of environmental conditions, fertilizers, irrigation, and adaption to climate change by selecting suitable varieties. In our BASE simulations, the combined effect is an average yield increase of ∼ 17 and ∼ 41 % (LPJG$_{IMAGE}$ and LPJG$_{MAgPIE}$) between 2000–2009 and 2090–2099. In the LUMs the mitigation scenarios are characterized by additional yield increases compared to BASE, triggered by increased land prices. This intensification is to some extent reflected in the fertilizer rates (derived from yields) provided by the LUMs; however, other management improvements and investments in research and development leading to higher-yielding varieties also impact future yield increases. Additional assumptions about yield increases driven by technological progress can thus not be captured by LPJ-GUESS. The simulated decline in productivity in response to shrinking cropland area in the mitigation scenarios suggests that, when adapting N fertilization, irrigation and cropland area, and location from the LUMs, additional yield increases of up to 6.6 and 35 % (LPJG$_{IMAGE}$ and LPJG$_{MAgPIE}$) would be required between the 2000s and the 2090s to produce the same amount of food crops as in the BASE scenario, equivalent to ∼ 0.07 and 0.33 % per year.

4.5 Water and air quality

Managed agricultural systems directly impact freshwater quality. Historically, approximately 20 % of reactive N

moved into aquatic ecosystems (Galloway et al., 2004), causing drinking water pollution and eutrophication. As N loss in LPJ-GUESS is largely driven by fertilization (Blanke et al., 2017), the much higher future fertilization rates compared to present-day ($+78\%$ for $\text{LPJG}_{\text{IMAGE}}$; $+95\%$ for $\text{LPJG}_{\text{MAgPIE}}$) lead to an increase in N loss of 82 and 62 % in BASE. Such a large increase would have severe impacts on waterways and coastal zones, where current levels of N pollution are already having substantial effects (Camargo and Alonso, 2006). However, as discussed above, the N application rates are derived from crop yields in the LUMs, and can only be partially utilized by LPJ-GUESS due to its lower yield levels. Increasing crop yields by increased N inputs leads to a strong decline in nutrient use efficiency and declining returns on yields (Cassman et al., 2002; Mueller et al., 2017). In contrast to the BASE simulations, the mitigation simulations result in somewhat lower N losses because less fertilizer is applied (ADAFF) or because bioenergy harvest removes more N than is added via bioenergy crop fertilization (BECCS). Simulated N losses in LPJ-GUESS are affected by different assumptions about N fertilizers and inconsistencies between the models: fertilizer rates in the LUMs were calculated to support the estimated crop yields (and hence the ensuing N demand). The resulting grid-cell averages available to LPJ-GUESS did not take into account differences in N application across crop types in a grid cell (Mueller et al., 2012). Additionally, IMAGE and MAgPIE simulate further increases in crop productivity and N use efficiency and therefore nutrient recovery in harvested biomass, which may only be partly captured by LPJ-GUESS (see Sect. 4.4).

Although we do not explicitly simulate emissions of N gases, increased N losses suggest an excess of soil N, which increases the likelihood of gaseous reactive N emissions such as NO_X and ammonia (NH_3) pollution, contributing to particulate matter formation, visibility degradation, and atmospheric N deposition (Behera et al., 2013). The chemical form and level of these emissions will strongly depend on soil water status (Liu et al., 2007). Improvements in air quality, e.g. via reductions in tropospheric ozone (O_3), are not only relevant for human health but can also enhance plant productivity and crop yields (Wilkinson et al., 2012). The response of O_3 to BVOC emissions changes depends on the local $NO_X : BVOC$ ratio (Sillman, 1999). An increase in BVOC emissions slightly suppresses O_3 concentration in regions of low NO_X background but promotes it in polluted regions (Pyle et al., 2011). Ganzeveld et al. (2010) used a chemistry–climate model to study the effects of LUC in the SRES A2 scenario (tropical deforestation) on atmospheric chemistry. By year 2050, they found increases in boundary layer ozone mixing ratios of up to 9 ppb (20 %). Changes in the concentration of the hydroxyl radical resulting from deforestation (the primary atmospheric oxidant, and main determinant of atmospheric methane lifetime) are much less clear due to uncertainties in isoprene oxidation chemistry

(Fuchs et al., 2013; Hansen et al., 2017; Lelieveld et al., 2008), but O_3 concentrations were not sensitive to this uncertainty (Pugh et al., 2010). ADAFF describes a reverse scenario, with forest expansion being largely concentrated in the tropics. The sign of changes in the ADAFF simulations is reverse to changes in Ganzeveld et al. (2010): by mid-century, global N loss in ADAFF decreases by ~ 8 and 4 % and isoprene emissions increase by ~ 14 and 4 % compared to BASE. Consequently, we would expect tropospheric O_3 burden in ADAFF to decrease in the tropics but to increase in large parts of the mid-latitudes. However, changes in overall air quality will likely be dominated by anthropogenic emissions rather than LUC (Val Martin et al., 2015). BVOC emissions might also increase in bioenergy scenarios (Rosenkranz et al., 2015) but this does not happen in our study as the LUMs assumed grasses to be the predominant bioenergy crop.

4.6 Potential impacts on biodiversity

Global-scale approaches that link changes in LU, climate, and other drivers to effects on biodiversity are scarce, and burdened with high uncertainty, though some approaches exist (Alkemade et al., 2009; Visconti et al., 2011). Biodiversity, whether it is being perceived as a requisite for the provision of ESs or an ES per se, with its own intrinsic value (Liang et al., 2016; Mace et al., 2012), has not been considered in our analysis. Nevertheless, it is evident that biodiversity can be in critical conflict with demands for land resources such as food or timber (Behrman et al., 2015; Murphy and Romanuk, 2014). LUC has been the most critical driver of recent species loss (Jantz et al., 2015; Newbold et al., 2014). This has led to substantial concerns that land requirements for bioenergy crops would be competing with conservation areas directly or by leakage. Santangeli et al. (2016) found around half of today's global bioenergy production potential to be located either in already protected areas or in land that has highest priority for protection, indicating a high risk for biodiversity in the absence of strong regulatory conservation efforts.

In principle, avoided deforestation and reforestation/afforestation should maintain and enhance habitat and species richness, since forests are amongst the most diverse ecosystems (Liang et al., 2016). Forestation could also support the restoration of degraded ecosystems. However, success of large-scale reforestation–afforestation programs under a C-uptake as well as a biodiversity perspective will depend critically on the types of forests promoted and so far show mixed results (Cunningham et al., 2015; Hua et al., 2016). Likewise, even under a globally implemented forest conservation scheme there may be cropland expansion into non-forested regions that could well be C-rich (implying reduced overall C mitigation) but also diverse such as savannas or natural grasslands.

4.7 Role of model assumptions on carbon uptake via land-based mitigation and implications for other ecosystem services

Our simulations show that trade-offs between C uptake and other ESs are to be expected. Consequently, the question of whether land-based mitigation projects should be realized depends not only on the effects on ESs, but also on the magnitude of C uptake that will be achieved. However, our study suggests that potential C uptake is highly model-dependent: C uptake in the three land-based mitigation options in LPJ-GUESS is lower than the target value used in the LUMs. When the underlying reasons for model–model discrepancies are explored, a number of reasons can be identified such as bioenergy yields, forest regrowth, legacy effects from past LUC, and recovery of soil carbon in response to reforestation. Additionally, in the BECCS scenarios, the CDR target was implemented as a CCS target which does not account for additional LUC emissions, partly explaining the lower CDR values.

For forest regrowth, the current model configuration of LPJ-GUESS simulates natural forest succession, including the representation of different age classes. Krause et al. (2016) showed that the recovery of C in ecosystems following different agricultural LU histories broadly agreed with site-based measurements. LPJ-GUESS also has N (and soil water availability) as an explicit constraint on forest growth and has been successfully tested against a broad range of observations (Fleischer et al., 2015; Smith et al., 2014). These studies indicate an overall realistic rate of forest growth under natural succession. However, much of the afforestation may occur with management facilitating fast built-up of C stocks (as assumed in MAgPIE), but LPJ-GUESS does not implement plantations and has thus not been evaluated against this type of regrowth. Forest (re)growth is simulated very differently in LPJ-GUESS (where different age classes and their competition are simulated), IMAGE (where in this study the dynamically coupled LPJmL DGVM simulates natural regrowth in one individual per PFT) and MAgPIE (where managed regrowth is prescribed towards potential C densities from LPJmL, see Sect. 2.2). LPJmL also does not yet consider N constraints on vegetation regrowth. C losses from deforestation and maximum C uptake following reforestation depend on potential C densities which are likely different in LPJmL and LPJ-GUESS. In the LUMs, the model's algorithm adopts C pools from LPJmL and can thus decide to reforest the most suitable areas, while in LPJ-GUESS other regions might have more reforestation potential. Finally, soil C sequestration rates are likely different between LPJ-GUESS and LPJmL, especially for MAgPIE-LPJmL where the assumption of soil C recovering within 20 years is likely overoptimistic (see Krause et al., 2016).

For BECCS, LPJ-GUESS simulates CCS rates of ~ 2.2 and $1.8\,\mathrm{GtC\,yr^{-1}}$ (LPJG$_{\mathrm{IMAGE}}$ and LPJG$_{\mathrm{MAgPIE}}$) by the end of the 21st century, compared to $\sim 2.8\,\mathrm{GtC\,yr^{-1}}$ reported from the LUMs directly. The number from the LUMs is close to the mean removal rate of $3.3\,\mathrm{GtC\,yr^{-1}}$ reported in Smith et al. (2016) for scenarios of similar production area (380–700, vs. 493 and 363 Mha in our IMAGE and MAgPIE BECCS scenarios, respectively) and slightly larger CO_2 concentrations (430–480 ppmv vs. 424 ppmv). Discrepancies between the models arise mainly from differences in assumptions about bioenergy crop yields. In our LPJ-GUESS simulations we grew bioenergy crops as corn (i.e. a crop functional type with parameters taken from corn). By the end of the century, simulated bioenergy yields are higher for LPJG$_{\mathrm{MAgPIE}}$ BECCS (on average $13.8\,\mathrm{t\,dry\,mass\,ha^{-1}\,yr^{-1}}$, 10 % of total above-ground biomass remaining on-site) than for LPJG$_{\mathrm{IMAGE}}$ BECCS ($12.2\,\mathrm{t\,dry\,mass\,ha^{-1}\,yr^{-1}}$) due to different fertilizer rates and production locations. Bioenergy crop yields in LPJ-GUESS might be influenced by inconsistencies between the models about fertilization of bioenergy crops: while the LUMs generally assume high N application, fertilizer rates are reduced in areas used for bioenergy production because bioenergy crops are less N-demanding. Consequently, the fertilizer rates from the LUMs might be insufficient to fulfil the N demand of the corn-based bioenergy crop in LPJ-GUESS, which responds strongly to fertilization (Blanke et al., 2017). In contrast, bioenergy crops in the LUMs are represented by dedicated lignocellulosic energy grasses. Reported yields of dedicated bioenergy crops under present-day conditions show large variability (*miscanthus × giganteus*: 5–44 t dry mass ha^{-1} yr^{-1}; switchgrass: 1–35 t ha^{-1} yr^{-1}; woody species: 0–51 t ha^{-1} yr^{-1}), depending on location, plot size, and management (Searle and Malins, 2014). By the end of the century, the LUMs report average bioenergy yields of $\sim 15.0\,\mathrm{t\,ha^{-1}\,yr^{-1}}$ (IMAGE) and $\sim 20.3\,\mathrm{t\,ha^{-1}\,yr^{-1}}$ (MAgPIE), but how bioenergy yields will evolve in reality when averaged across regions (including more marginal land) is highly uncertain (Creutzig, 2016; Searle and Malins, 2014; Slade et al., 2014).

Legacy effects from historic LU might also impact future C uptake as the soil C balance continues to respond to LUC decades or even centuries after (Krause et al., 2016; Pugh et al., 2015). We assessed the contribution of legacy effects by comparing an LPJ-GUESS simulation in which LU (but not climate and CO_2) was held constant from year 1970 for IMAGE and 1995 for MAgPIE (consistent with the scenario starting years in each model) with a run with fixed LU from year 1901 on. The differences then seen over the 21st century between these two simulations would arise chiefly from legacy fluxes of 20th century LUC. These were found to be ~ 17–$18\,\mathrm{GtC}$ (not shown), accounting for part of the difference in uptake between LPJ-GUESS and the LUMs. In the LUMs, harmonization to history has been done with respect to land cover, but this was not possible with respect to changes in vegetation and soil C pools (prior to 1970/1995).

Our results show that assumptions about forest growth and C densities, bioenergy crop yields, and timescales of

soil processes can critically influence the C removal potential of land-based mitigation. Large uncertainties about forest regrowth trajectories in different DGVMs (Pongratz et al., in preparation) and BECCS potential to remove C from the atmosphere (Creutzig et al., 2015; Kemper, 2015) have been reported before, including the importance of second-generation bioenergy crops (Kato and Yamagata, 2014) and LU-driven C losses in vegetation and soils (Wiltshire and Davies-Barnard, 2015). This is clearly an important subject for future research. Additional analyses about the difference in C removal between the LUMs and LPJ-GUESS, including results from additional DGVMs, are ongoing and will be published in a separate paper (Krause et al., 2017).

5   Conclusions

Terrestrial ecosystems provide us with many valuable services like climate and air quality regulation, water and food provision, or flood protection. While substantial changes in ecosystem functions are likely to occur within the 21st century even in the absence of land-based climate change mitigation, additional impacts are to be expected from land management for negative emissions. In all mitigation simulations, what might generally be perceived as beneficial effects on some ecosystem functions and their services (e.g. decreased N loss improving water and air quality) were counteracted by negative effects on others (e.g. reduced crop production), including substantial temporal and regional variations. Environmental side effects in our ADAFF simulations were usually larger than in BECCS, presumably reflecting the larger area affected by land-cover transitions in ADAFF. Without a valuation exercise it is not possible to state whether one option would be "better" than the other. All mitigation approaches might reduce crop production (in the absence of assumptions about large technology-related yield increases) but potentially improve air and water quality via reduced N loss. Impacts on climate via biophysical effects and on water availability and flood risks via changes in runoff were found to be relatively small in terms of percentage changes when averaged over large areas, but this does not exclude the possibility of significant impacts, e.g. on the scale of large catchments.

Policy makers should be aware of manifold side effects – be they positive or negative – when discussing and evaluating the feasibility and effects of different climate mitigation options, possibly involving the prioritization of individual ESs at the costs of exacerbating other challenges. Our analysis makes some of these trade-offs explicit, but there are many other services offered by ecosystems much more difficult to quantify, particularly relating to cultural services, which also need to be considered. Any discussion about land-based climate mitigation efforts should take into account their effects on ESs beyond C storage in order to avoid unintended negative consequences, which would be intrinsically undesirable

and may also affect the effective delivery of climate mitigation through societal feedbacks.

The Supplement related to this article is available online at https://doi.org/10.5194/bg-14-4829-2017-supplement.

References

Ahlstrom, A., Schurgers, G., Arneth, A., and Smith, B.: Robustness and uncertainty in terrestrial ecosystem carbon response to CMIP5 climate change projections, Environ. Res. Lett., 7, 044008, https://doi.org/10.1088/1748-9326/7/4/044008, 2012.

Alexander, P., Prestele, R., Verburg, P. H., Arneth, A., Baranzelli, C., Silva, F. B. E., Brown, C., Butler, A., Calvin, K., Dendoncker, N., Doelman, J. C., Dunford, R., Engstrom, K., Eitelberg, D., Fujimori, S., Harrison, P. A., Hasegawa, T., Havlik, P., Holzhauer, S., Humpenoder, F., Jacobs-Crisioni, C., Jain, A. K., Krisztin, T., Kyle, P., Lavalle, C., Lenton, T., Liu, J. Y., Meiyappan, P., Popp, A., Powell, T., Sands, R. D., Schaldach, R., Stehfest, E., Steinbuks, J., Tabeau, A., van Meijl, H.,

Wise, M. A., and Rounsevell, M. D. A.: Assessing uncertainties in land cover projections, Glob. Change Biol., 23, 767–781, https://doi.org/10.1111/gcb.13447, 2017.

Alkama, R. and Cescatti, A.: Biophysical climate impacts of recent changes in global forest cover, Science, 351, 600–604, https://doi.org/10.1126/science.aac8083, 2016.

Alkemade, R., van Oorschot, M., Miles, L., Nellemann, C., Bakkenes, M., and ten Brink, B.: GLOBIO3: A framework to investigate options for reducing global terrestrial biodiversity loss, Ecosystems, 12, 374–390, https://doi.org/10.1007/s10021-009-9229-5, 2009.

Anderson, K. and Peters, G.: The trouble with negative emissions, Science, 354, 182–183, https://doi.org/10.1126/science.aah4567, 2016.

Arneth, A., Niinemets, Ü., Pressley, S., Bäck, J., Hari, P., Karl, T., Noe, S., Prentice, I. C., Serça, D., Hickler, T., Wolf, A., and Smith, B.: Process-based estimates of terrestrial ecosystem isoprene emissions: incorporating the effects of a direct CO_2-isoprene interaction, Atmos. Chem. Phys., 7, 31–53, https://doi.org/10.5194/acp-7-31-2007, 2007.

Arneth, A., Harrison, S. P., Zaehle, S., Tsigaridis, K., Menon, S., Bartlein, P. J., Feichter, J., Korhola, A., Kulmala, M., O'Donnell, D., Schurgers, G., Sorvari, S., and Vesala, T.: Terrestrial biogeochemical feedbacks in the climate system, Nat. Geosci., 3, 525–532, https://doi.org/10.1038/ngeo905, 2010.

Bala, G., Caldeira, K., Wickett, M., Phillips, T. J., Lobell, D. B., Delire, C., and Mirin, A.: Combined climate and carbon-cycle effects of large-scale deforestation, P. Natl. Acad. Sci. USA, 104, 6550–6555, https://doi.org/10.1073/pnas.0608998104, 2007.

Ban-Weiss, G. A., Bala, G., Cao, L., Pongratz, J., and Caldeira, K.: Climate forcing and response to idealized changes in surface latent and sensible heat, Environ. Res. Lett., 6, 034032, https://doi.org/10.1088/1748-9326/6/3/034032, 2011.

Bathiany, S., Claussen, M., Brovkin, V., Raddatz, T., and Gayler, V.: Combined biogeophysical and biogeochemical effects of large-scale forest cover changes in the MPI earth system model, Biogeosciences, 7, 1383–1399, https://doi.org/10.5194/bg-7-1383-2010, 2010.

Behera, S. N., Sharma, M., Aneja, V. P., and Balasubramanian, R.: Ammonia in the atmosphere: a review on emission sources, atmospheric chemistry and deposition on terrestrial bodies, Environ. Sci. Pollut. R., 20, 8092–8131, https://doi.org/10.1007/s11356-013-2051-9, 2013.

Behrman, K. D., Juenger, T. E., Kiniry, J. R., and Keitt, T. H.: Spatial land use trade-offs for maintenance of biodiversity, biofuel, and agriculture, Landscape Ecol., 30, 1987–1999, https://doi.org/10.1007/s10980-015-0225-1, 2015.

Bennett, E. M., Peterson, G. D., and Gordon, L. J.: Understanding relationships among multiple ecosystem services, Ecol. Lett., 12, 1394–1404, https://doi.org/10.1111/j.1461-0248.2009.01387.x, 2009.

Betts, R. A.: Offset of the potential carbon sink from boreal forestation by decreases in surface albedo, Nature, 408, 187–190, https://doi.org/10.1038/35041545, 2000.

Blanke, J. H., Olin, S., Stürck, J., Sahlin, U., Lindeskog, M., Helming, J., and Lehsten, V.: Assessing the impact of changes in land-use intensity and climate on simulated trade-offs between crop yield and nitrogen leaching, Agr. Ecosyst. Environ., 239, 385–398, https://doi.org/10.1016/j.agee.2017.01.038, 2017.

Boisier, J. P., de Noblet-Ducoudré, N., and Ciais, P.: Inferring past land use-induced changes in surface albedo from satellite observations: a useful tool to evaluate model simulations, Biogeosciences, 10, 1501–1516, https://doi.org/10.5194/bg-10-1501-2013, 2013.

Bondeau, A., Smith, P. C., Zaehle, S., Schaphoff, S., Lucht, W., Cramer, W., Gerten, D., Lotze-Campen, H., Muller, C., Reichstein, M., and Smith, B.: Modelling the role of agriculture for the 20th century global terrestrial carbon balance, Glob. Change Biol., 13, 679–706, https://doi.org/10.1111/j.1365-2486.2006.01305.x, 2007.

Boucher, O., Myhre, G., and Myhre, A.: Direct human influence of irrigation on atmospheric water vapour and climate, Clim. Dynam., 22, 597–603, https://doi.org/10.1007/s00382-004-0402-4, 2004.

Boysen, L. R., Lucht, W., and Gerten, D.: Trade-offs for food production, nature conservation and climate limit the terrestrial carbon dioxide removal potential, Glob. Change Biol., 23, 4303–4317, https://doi.org/10.1111/gcb.13745, 2017.

Bradshaw, C. J. A., Sodhi, N. S., Peh, K. S. H., and Brook, B. W.: Global evidence that deforestation amplifies flood risk and severity in the developing world, Glob. Change Biol., 13, 2379–2395, https://doi.org/10.1111/j.1365-2486.2007.01446.x, 2007.

Camargo, J. A. and Alonso, A.: Ecological and toxicological effects of inorganic nitrogen pollution in aquatic ecosystems: A global assessment, Environ. Int., 32, 831–849, https://doi.org/10.1016/j.envint.2006.05.002, 2006.

Carslaw, K. S., Boucher, O., Spracklen, D. V., Mann, G. W., Rae, J. G. L., Woodward, S., and Kulmala, M.: A review of natural aerosol interactions and feedbacks within the Earth system, Atmos. Chem. Phys., 10, 1701–1737, https://doi.org/10.5194/acp-10-1701-2010, 2010.

Cassman, K. G., Dobermann, A., and Walters, D. T.: Agroecosystems, nitrogen-use efficiency, and nitrogen management, Ambio, 31, 132–140, https://doi.org/10.1639/0044-7447(2002)031[0132:Anuean]2.0.Co;2, 2002.

Creutzig, F.: Economic and ecological views on climate change mitigation with bioenergy and negative emissions, Gcb Bioenergy, 8, 4–10, https://doi.org/10.1111/gcbb.12235, 2016.

Creutzig, F., Ravindranath, N. H., Berndes, G., Bolwig, S., Bright, R., Cherubini, F., Chum, H., Corbera, E., Delucchi, M., Faaij, A., Fargione, J., Haberl, H., Heath, G., Lucon, O., Plevin, R., Popp, A., Robledo-Abad, C., Rose, S., Smith, P., Stromman, A., Suh, S., and Masera, O.: Bioenergy and climate change mitigation: an assessment, Gcb Bioenergy, 7, 916–944, https://doi.org/10.1111/gcbb.12205, 2015.

Crutzen, P. J., Mosier, A. R., Smith, K. A., and Winiwarter, W.: N_2O release from agro-biofuel production negates global warming reduction by replacing fossil fuels, Atmos. Chem. Phys., 8, 389–395, https://doi.org/10.5194/acp-8-389-2008, 2008.

Cunningham, S. C., Mac Nally, R., Baker, P. J., Cavagnaro, T. R., Beringer, J., Thomson, J. R., and Thompson, R. M.: Balancing the environmental benefits of reforestation in agricultural regions, Perspect. Plant Ecol., 17, 301–317, https://doi.org/10.1016/j.ppees.2015.06.001, 2015.

Davidson, E. A. and Kanter, D.: Inventories and scenarios of nitrous oxide emissions, Environ. Res. Lett., 9, 105012, https://doi.org/10.1088/1748-9326/9/10/105012, 2014.

Davies-Barnard, T., Valdes, P. J., Singarayer, J. S., Pacifico, F. M., and Jones, C. D.: Full effects of land use change in the representative concentration pathways, Environ. Res. Lett., 9, 114014, https://doi.org/10.1088/1748-9326/9/11/114014, 2014.

DeFries, R. S., Foley, J. A., and Asner, G. P.: Land-use choices: balancing human needs and ecosystem function, Front. Ecol. Environ., 2, 249–257, https://doi.org/10.1890/1540-9295(2004)002[0249:Lcbhna]2.0.Co;2, 2004.

Dellink, R., Chateau, J., Lanzi, E., and Magne, B.: Long-term economic growth projections in the Shared Socioeconomic Pathways, Global Environ. Chang., 42, 200–214, https://doi.org/10.1016/j.gloenvcha.2015.06.004, 2017.

de Noblet-Ducoudre, N., Boisier, J. P., Pitman, A., Bonan, G. B., Brovkin, V., Cruz, F., Delire, C., Gayler, V., van den Hurk, B. J. J. M., Lawrence, P. J., van der Molen, M. K., Muller, C., Reick, C. H., Strengers, B. J., and Voldoire, A.: Determining Robust Impacts of Land-Use-Induced Land Cover Changes on Surface Climate over North America and Eurasia: Results from the First Set of LUCID Experiments, J Climate, 25, 3261–3281, https://doi.org/10.1175/Jcli-D-11-00338.1, 2012.

Doelman, J. C., Stehfest, E., Tabeau, A., van Meijl, H., Lassaletta, L., Gernaat, D. E. H. J., Neumann-Hermans, K., Harmsen, M., Daioglou, V., Biemans, H., van der Sluis, S., and van Vuuren, D. P.: Exploring SSP land-use dynamics using the IMAGE model: regional and gridded scenarios of land-use change and land-based climate change mitigation, submitted to Global Environ. Chang., 2017.

Elliott, J., Deryng, D., Mueller, C., Frieler, K., Konzmann, M., Gerten, D., Glotter, M., Florke, M., Wada, Y., Best, N., Eisner, S., Fekete, B. M., Folberth, C., Foster, I., Gosling, S. N., Haddeland, I., Khabarov, N., Ludwig, F., Masaki, Y., Olin, S., Rosenzweig, C., Ruane, A. C., Satoh, Y., Schmid, E., Stacke, T., Tang, Q. H., and Wisser, D.: Constraints and potentials of future irrigation water availability on agricultural production under climate change, P. Natl. Acad. Sci. USA, 111, 3239–3244, https://doi.org/10.1073/pnas.1222474110, 2014.

Ellison, D., Futter, M. N., and Bishop, K.: On the forest cover-water yield debate: from demand- to supply-side thinking, Glob. Change Biol., 18, 806–820, https://doi.org/10.1111/j.1365-2486.2011.02589.x, 2012.

Erisman, J. W., Galloway, J., Seitzinger, S., Bleeker, A., and Butterbach-Bahl, K.: Reactive nitrogen in the environment and its effect on climate change, Curr. Opin. Env. Sust., 3, 281–290, https://doi.org/10.1016/j.cosust.2011.08.012, 2011.

Farley, K. A., Jobbagy, E. G., and Jackson, R. B.: Effects of afforestation on water yield: a global synthesis with implications for policy, Glob. Change Biol., 11, 1565–1576, https://doi.org/10.1111/j.1365-2486.2005.01011.x, 2005.

Ferreira, S. and Ghimire, R.: Forest cover, socioeconomics, and reported flood frequency in developing countries, Water Resour. Res., 48, W08529, https://doi.org/10.1029/2011wr011701, 2012.

Fleischer, K., Warlind, D., van der Molen, M. K., Rebel, K. T., Arneth, A., Erisman, J. W., Wassen, M. J., Smith, B., Gough, C. M., Margolis, H. A., Cescatti, A., Montagnani, L., Arain, A., and Dolman, A. J.: Low historical nitrogen deposition effect on carbon sequestration in the boreal zone, J. Geophys. Res.-Biogeo., 120, 2542–2561, https://doi.org/10.1002/2015JG002988, 2015.

Foley, J. A., DeFries, R., Asner, G. P., Barford, C., Bonan, G., Carpenter, S. R., Chapin, F. S., Coe, M. T., Daily, G. C., Gibbs, H. K., Helkowski, J. H., Holloway, T., Howard, E. A., Kucharik, C. J., Monfreda, C., Patz, J. A., Prentice, I. C., Ramankutty, N., and Snyder, P. K.: Global consequences of land use, Science, 309, 570–574, https://doi.org/10.1126/science.1111772, 2005.

Friedlingstein, P., Meinshausen, M., Arora, V. K., Jones, C. D., Anav, A., Liddicoat, S. K., and Knutti, R.: Uncertainties in CMIP5 Climate Projections due to Carbon Cycle Feedbacks, J. Climate, 27, 511–526, https://doi.org/10.1175/Jcli-D-12-00579.1, 2014.

Fuchs, H., Hofzumahaus, A., Rohrer, F., Bohn, B., Brauers, T., Dorn, H. P., Haseler, R., Holland, F., Kaminski, M., Li, X., Lu, K., Nehr, S., Tillmann, R., Wegener, R., and Wahner, A.: Experimental evidence for efficient hydroxyl radical regeneration in isoprene oxidation, Nat. Geosci., 6, 1023–1026, https://doi.org/10.1038/NGEO1964, 2013.

Fuss, S., Canadell, J. G., Peters, G. P., Tavoni, M., Andrew, R. M., Ciais, P., Jackson, R. B., Jones, C. D., Kraxner, F., Nakicenovic, N., Le Quere, C., Raupach, M. R., Sharifi, A., Smith, P., and Yamagata, Y.: COMMENTARY: Betting on negative emissions, Nat. Clim. Change, 4, 850–853, https://doi.org/10.1038/nclimate2392, 2014.

Galloway, J. N., Dentener, F. J., Capone, D. G., Boyer, E. W., Howarth, R. W., Seitzinger, S. P., Asner, G. P., Cleveland, C. C., Green, P. A., Holland, E. A., Karl, D. M., Michaels, A. F., Porter, J. H., Townsend, A. R., and Vorosmarty, C. J.: Nitrogen cycles: past, present, and future, Biogeochemistry, 70, 153–226, https://doi.org/10.1007/s10533-004-0370-0, 2004.

Ganzeveld, L., Bouwman, L., Stehfest, E., van Vuuren, D. P., Eickhout, B., and Lelieveld, J.: Impact of future land use and land cover changes on atmospheric chemistry-climate interactions, J. Geophys. Res.-Atmos., 115, D23301, https://doi.org/10.1029/2010jd014041, 2010.

Gerten, D., Schaphoff, S., Haberlandt, U., Lucht, W., and Sitch, S.: Terrestrial vegetation and water balance – hydrological evaluation of a dynamic global vegetation model, J. Hydrol., 286, 249–270, https://doi.org/10.1016/j.jhydrol.2003.09.029, 2004.

Giglio, L., Randerson, J. T., van der Werf, G. R., Kasibhatla, P. S., Collatz, G. J., Morton, D. C., and DeFries, R. S.: Assessing variability and long-term trends in burned area by merging multiple satellite fire products, Biogeosciences, 7, 1171–1186, https://doi.org/10.5194/bg-7-1171-2010, 2010.

Hallgren, W., Schlosser, C. A., Monier, E., Kicklighter, D., Sokolov, A., and Melillo, J.: Climate impacts of a large-scale biofuels expansion, Geophys. Res. Lett., 40, 1624–1630, https://doi.org/10.1002/grl.50352, 2013.

Hansen, R. F., Lewis, T. R., Graham, L., Whalley, S. K., Seakins, P. W., Heard, D. E., and Blitz, M. A.: OH production from the photolysis of isoprene-derived peroxy radicals: cross-sections, quantum yields and atmospheric implications, Phys. Chem. Chem. Phys, 19, 2332–2345, https://doi.org/10.1039/c6cp06718b, 2017.

Hantson, S., Knorr, W., Schurgers, G., Pugh, T. A. M., and Arneth, A.: Global isoprene and monoterpene emissions under changing climate, vegetation, CO_2 and land use, Atmos. Environ., 155, 35–45, https://doi.org/10.1016/j.atmosenv.2017.02.010, 2017.

Hempel, S., Frieler, K., Warszawski, L., Schewe, J., and Piontek, F.: A trend-preserving bias correction –the ISI-MIP approach, Earth Syst. Dynam., 4, 219–236, https://doi.org/10.5194/esd-4-219-2013, 2013.

Hoogwijk, M., Faaija, A., van den Broek, R., Berndes, G., Gielen, D., and Turkenburg, W.: Exploration of the ranges of the global potential of biomass for energy, Biomass Bioenerg., 25, 119–133, https://doi.org/10.1016/S0961-9534(02)00191-5, 2003.

Hua, F. Y., Wang, X. Y., Zheng, X. L., Fisher, B., Wang, L., Zhu, J. G., Tang, Y., Yu, D. W., and Wilcove, D. S.: Opportunities for biodiversity gains under the world's largest reforestation programme, Nat. Commun., 7, 12717, https://doi.org/10.1038/Ncomms12717, 2016.

Humpenöder, F., Popp, A., Dietrich, J. P., Klein, D., Lotze-Campen, H., Bonsch, M., Bodirsky, B. L., Weindl, I., Stevanovic, M., and Muller, C.: Investigating afforestation and bioenergy CCS as climate change mitigation strategies, Environ. Res. Lett., 9, 064029, https://doi.org/10.1088/1748-9326/9/6/064029, 2014.

Jackson, R. B., Jobbagy, E. G., Avissar, R., Roy, S. B., Barrett, D. J., Cook, C. W., Farley, K. A., le Maitre, D. C., McCarl, B. A., and Murray, B. C.: Trading water for carbon with biological sequestration, Science, 310, 1944–1947, https://doi.org/10.1126/science.1119282, 2005.

Jantz, S. M., Barker, B., Brooks, T. M., Chini, L. P., Huang, Q. Y., Moore, R. M., Noel, J., and Hurtt, G. C.: Future habitat loss and extinctions driven by land-use change in biodiversity hotspots under four scenarios of climate-change mitigation, Conserv. Biol., 29, 1122–1131, https://doi.org/10.1111/cobi.12549, 2015.

Kato, E. and Yamagata, Y.: BECCS capability of dedicated bioenergy crops under a future land-use scenario targeting net negative carbon emissions, Earths Future, 2, 421–439, https://doi.org/10.1002/2014EF000249, 2014.

Keller, D. P., Feng, E. Y., and Oschlies, A.: Potential climate engineering effectiveness and side effects during a high carbon dioxide-emission scenario, Nat. Commun., 5, 3304, https://doi.org/10.1038/ncomms4304, 2014.

Kelley, D. I., Prentice, I. C., Harrison, S. P., Wang, H., Simard, M., Fisher, J. B., and Willis, K. O.: A comprehensive benchmarking system for evaluating global vegetation models, Biogeosciences, 10, 3313–3340, https://doi.org/10.5194/bg-10-3313-2013, 2013.

Kemper, J.: Biomass and carbon dioxide capture and storage: A review, Int. J. Greenh. Gas Con., 40, 401–430, https://doi.org/10.1016/j.ijggc.2015.06.012, 2015.

Klein Goldewijk, K., Beusen, A., van Drecht, G., and de Vos, M.: The HYDE 3.1 spatially explicit database of human-induced global land-use change over the past 12,000 years, Global Ecol. Biogeogr., 20, 73–86, https://doi.org/10.1111/j.1466-8238.2010.00587.x, 2011.

Krause, A., Pugh, T. A. M., Bayer, A. D., Lindeskog, M., and Arneth, A.: Impacts of land-use history on the recovery of ecosystems after agricultural abandonment, Earth Syst. Dynam., 7, 745–766, https://doi.org/10.5194/esd-7-745-2016, 2016.

Krause, A., Pugh, T. A. M., Bayer, A. D., Li, W., Leung, F., Bondeau, A., Doelman, J. C., Humpenöder, F., Anthoni, P., Bodirsky, B. L., Ciais, P., Müller, C., Murray-Tortarolo, G., Olin, S., Popp, A., Sitch, S., Stehfest, E., and Arneth, A.: Large uncertainty in carbon uptake potential of land-based climate change mitigation efforts, in preparation, 2017.

Lamarque, J.-F., Bond, T. C., Eyring, V., Granier, C., Heil, A., Klimont, Z., Lee, D., Liousse, C., Mieville, A., Owen, B., Schultz, M. G., Shindell, D., Smith, S. J., Stehfest, E., Van Aardenne, J., Cooper, O. R., Kainuma, M., Mahowald, N., McConnell, J. R., Naik, V., Riahi, K., and van Vuuren, D. P.: Historical (1850–2000) gridded anthropogenic and biomass burning emissions of reactive gases and aerosols: methodology and application, Atmos. Chem. Phys., 10, 7017–7039, https://doi.org/10.5194/acp-10-7017-2010, 2010.

Lamarque, J. F., Kyle, G. P., Meinshausen, M., Riahi, K., Smith, S. J., van Vuuren, D. P., Conley, A. J., and Vitt, F.: Global and regional evolution of short-lived radiatively-active gases and aerosols in the Representative Concentration Pathways, Climatic Change, 109, 191–212, https://doi.org/10.1007/s10584-011-0155-0, 2011.

Lelieveld, J., Butler, T. M., Crowley, J. N., Dillon, T. J., Fischer, H., Ganzeveld, L., Harder, H., Lawrence, M. G., Martinez, M., Taraborrelli, D., and Williams, J.: Atmospheric oxidation capacity sustained by a tropical forest, Nature, 452, 737–740, https://doi.org/10.1038/nature06870, 2008.

Le Quéré, C., Moriarty, R., Andrew, R. M., Canadell, J. G., Sitch, S., Korsbakken, J. I., Friedlingstein, P., Peters, G. P., Andres, R. J., Boden, T. A., Houghton, R. A., House, J. I., Keeling, R. F., Tans, P., Arneth, A., Bakker, D. C. E., Barbero, L., Bopp, L., Chang, J., Chevallier, F., Chini, L. P., Ciais, P., Fader, M., Feely, R. A., Gkritzalis, T., Harris, I., Hauck, J., Ilyina, T., Jain, A. K., Kato, E., Kitidis, V., Klein Goldewijk, K., Koven, C., Landschützer, P., Lauvset, S. K., Lefèvre, N., Lenton, A., Lima, I. D., Metzl, N., Millero, F., Munro, D. R., Murata, A., Nabel, J. E. M. S., Nakaoka, S., Nojiri, Y., O'Brien, K., Olsen, A., Ono, T., Pérez, F. F., Pfeil, B., Pierrot, D., Poulter, B., Rehder, G., Rödenbeck, C., Saito, S., Schuster, U., Schwinger, J., Séférian, R., Steinhoff, T., Stocker, B. D., Sutton, A. J., Takahashi, T., Tilbrook, B., van der Laan-Luijkx, I. T., van der Werf, G. R., van Heuven, S., Vandemark, D., Viovy, N., Wiltshire, A., Zaehle, S., and Zeng, N.: Global Carbon Budget 2015, Earth Syst. Sci. Data, 7, 349–396, https://doi.org/10.5194/essd-7-349-2015, 2015.

Li, Y., Zhao, M. S., Motesharrei, S., Mu, Q. Z., Kalnay, E., and Li, S. C.: Local cooling and warming effects of forests based on satellite observations, Nat. Commun., 6, 6603, https://doi.org/10.1038/Ncomms7603, 2015.

Liang, J. J., Crowther, T. W., Picard, N., Wiser, S., Zhou, M., Alberti, G., Schulze, E. D., McGuire, A. D., Bozzato, F., Pretzsch, H., de-Miguel, S., Paquette, A., Herault, B., Scherer-Lorenzen, M., Barrett, C. B., Glick, H. B., Hengeveld, G. M., Nabuurs, G. J., Pfautsch, S., Viana, H., Vibrans, A. C., Ammer, C., Schall, P., Verbyla, D., Tchebakova, N., Fischer, M., Watson, J. V., Chen, H. Y. H., Lei, X. D., Schelhaas, M. J., Lu, H. C., Gianelle, D., Parfenova, E. I., Salas, C., Lee, E., Lee, B., Kim, H. S., Bruelheide, H., Coomes, D. A., Piotto, D., Sunderland, T., Schmid, B., Gourlet-Fleury, S., Sonke, B., Tavani, R., Zhu, J., Brandl, S., Vayreda, J., Kitahara, F., Searle, E. B., Neldner, V. J., Ngugi, M. R., Baraloto, C., Frizzera, L., Balazy, R., Oleksyn, J., Zawila-Niedzwiecki, T., Bouriaud, O., Bussotti, F., Finer, L., Jaroszewicz, B., Jucker, T., Valladares, F., Jagodzinski, A. M., Peri, P. L., Gonmadje, C., Marthy, W., O'Brien, T., Martin, E. H., Marshall, A. R., Rovero, F., Bitariho, R., Niklaus, P. A., Alvarez-Loayza, P., Chamuya, N., Valencia, R., Mortier, F., Wortel, V., Engone-Obiang, N. L., Ferreira, L. V., Odeke, D. E., Vasquez, R. M., Lewis, S. L., and Reich, P. B.: Positive biodiversity-productivity relationship predominant in global forests, Science, 354, 6309, https://doi.org/10.1126/science.aaf8957, 2016.

Lindeskog, M., Arneth, A., Bondeau, A., Waha, K., Seaquist, J., Olin, S., and Smith, B.: Implications of accounting for land use in simulations of ecosystem carbon cycling in Africa, Earth Syst. Dynam., 4, 385–407, https://doi.org/10.5194/esd-4-385-2013, 2013.

Liu, G. D., Li, Y. C., and Alva, A. K.: Moisture quotients for ammonia volatilization from four soils in potato production regions, Water Air Soil Poll., 183, 115–127, https://doi.org/10.1007/s11270-007-9361-9, 2007.

Lotze-Campen, H., Muller, C., Bondeau, A., Rost, S., Popp, A., and Lucht, W.: Global food demand, productivity growth, and the scarcity of land and water resources: a spatially explicit mathematical programming approach, Agr. Econ.-Blackwell, 39, 325–338, https://doi.org/10.1111/j.1574-0862.2008.00336.x, 2008.

Mace, G. M., Norris, K., and Fitter, A. H.: Biodiversity and ecosystem services: a multilayered relationship, Trends Ecol. Evol., 27, 19–26, https://doi.org/10.1016/j.tree.2011.08.006, 2012.

Meinshausen, M., Smith, S. J., Calvin, K., Daniel, J. S., Kainuma, M. L. T., Lamarque, J. F., Matsumoto, K., Montzka, S. A., Raper, S. C. B., Riahi, K., Thomson, A., Velders, G. J. M., and van Vuuren, D. P. P.: The RCP greenhouse gas concentrations and their extensions from 1765 to 2300, Climatic Change, 109, 213–241, https://doi.org/10.1007/s10584-011-0156-z, 2011.

Millennium Ecosystem Assessment (MEA): Ecosystems and Human Well-being: Synthesis, Washington, DC, USA, 155 pp., 2005.

Mueller, N. D., Gerber, J. S., Johnston, M., Ray, D. K., Ramankutty, N., and Foley, J. A.: Closing yield gaps through nutrient and water management, Nature, 490, 254–257, https://doi.org/10.1038/nature11420, 2012.

Mueller, N. D., Lassaletta, L., Runck, B. C., Billen, G., Garnier, J., and Gerber, J. S.: Declining spatial efficiency of global cropland nitrogen allocation, Global Biogeochem. Cy., 31, 245–257, https://doi.org/10.1002/2016GB005515, 2017.

Murphy, G. E. P. and Romanuk, T. N.: A meta-analysis of declines in local species richness from human disturbances, Ecol. Evol., 4, 91–103, https://doi.org/10.1002/ece3.909, 2014.

Newbold, T., Hudson, L. N., Phillips, H. R. P., Hill, S. L. L., Contu, S., Lysenko, I., Blandon, A., Butchart, S. H. M., Booth, H. L., Day, J., De Palma, A., Harrison, M. L. K., Kirkpatrick, L., Pynegar, E., Robinson, A., Simpson, J., Mace, G. M., Scharlemann, J. P. W., and Purvis, A.: A global model of the response of tropical and sub-tropical forest biodiversity to anthropogenic pressures, P. Roy. Soc. B-Biol. Sci., 281, 1792, https://doi.org/10.1098/Rspb.2014.1371, 2014.

Oki, T. and Kanae, S.: Global hydrological cycles and world water resources, Science, 313, 1068–1072, https://doi.org/10.1126/science.1128845, 2006.

Olin, S., Lindeskog, M., Pugh, T. A. M., Schurgers, G., Wårlind, D., Mishurov, M., Zaehle, S., Stocker, B. D., Smith, B., and Arneth, A.: Soil carbon management in large-scale Earth system modelling: implications for crop yields and nitrogen leaching, Earth Syst. Dynam., 6, 745–768, https://doi.org/10.5194/esd-6-745-2015, 2015a.

Olin, S., Schurgers, G., Lindeskog, M., Wårlind, D., Smith, B., Bodin, P., Holmér, J., and Arneth, A.: Modelling the response of yields and tissue C : N to changes in atmospheric CO_2 and N management in the main wheat regions of western Europe, Biogeosciences, 12, 2489–2515, https://doi.org/10.5194/bg-12-2489-2015, 2015b.

O'Neill, B. C., Kriegler, E., Riahi, K., Ebi, K. L., Hallegatte, S., Carter, T. R., Mathur, R., and van Vuuren, D. P.: A new scenario framework for climate change research: the concept of shared socioeconomic pathways, Climatic Change, 122, 387–400, https://doi.org/10.1007/s10584-013-0905-2, 2014.

Peters, G. P., Andrew, R. M., Boden, T., Canadell, J. G., Ciais, P., Le Quere, C., Marland, G., Raupach, M. R., and Wilson, C.: COMMENTARY: The challenge to keep global warming below 2 °C, Nat. Clim. Change, 3, 4–6, https://doi.org/10.1038/nclimate1783, 2013.

Peters, G. P., Andrew, R. M., Canadell, J. G., Fuss, S., Jackson, R. B., Korsbakken, J. I., Le Quere, C., and Nakicenovic, N.: Key indicators to track current progress and future ambition of the Paris Agreement, Nat. Clim. Change, 7, 118–123, https://doi.org/10.1038/Nclimate3202, 2017.

Piao, S. L., Sitch, S., Ciais, P., Friedlingstein, P., Peylin, P., Wang, X. H., Ahlstrom, A., Anav, A., Canadell, J. G., Cong, N., Huntingford, C., Jung, M., Levis, S., Levy, P. E., Li, J. S., Lin, X., Lomas, M. R., Lu, M., Luo, Y. Q., Ma, Y. C., Myneni, R. B., Poulter, B., Sun, Z. Z., Wang, T., Viovy, N., Zaehle, S., and Zeng, N.: Evaluation of terrestrial carbon cycle models for their response to climate variability and to CO_2 trends, Glob. Change Biol., 19, 2117–2132, https://doi.org/10.1111/gcb.12187, 2013.

Popp, A., Humpenoder, F., Weindl, I., Bodirsky, B. L., Bonsch, M., Lotze-Campen, H., Muller, C., Biewald, A., Rolinski, S., Stevanovic, M., and Dietrich, J. P.: Land-use protection for climate change mitigation, Nat. Clim. Change, 4, 1095–1098, https://doi.org/10.1038/Nclimate2444, 2014.

Popp, A., Calvin, K., Fujimori, S., Havlik, P., Humpenoder, F., Stehfest, E., Bodirsky, B. L., Dietrich, J. P., Doelmann, J. C., Gusti, M., Hasegawa, T., Kyle, P., Obersteiner, M., Tabeau, A., Takahashi, K., Valin, H., Waldhoff, S., Weindl, I., Wise, M., Kriegler, E., Lotze-Campen, H., Fricko, O., Riahi, K., and van Vuuren, D. P.: Land-use futures in the shared socio-economic pathways, Global Environ. Chang., 42, 331–345, https://doi.org/10.1016/j.gloenvcha.2016.10.002, 2017.

Posthumus, H., Morris, J., Hess, T. M., Neville, D., Phillips, E., and Baylis, A.: Impacts of the summer 2007 floods on agriculture in England, J. Flood Risk Manag., 2, 182–189, https://doi.org/10.1111/j.1753-318X.2009.01031.x, 2009.

Prestele, R., Alexander, P., Rounsevell, M. D. A., Arneth, A., Calvin, K., Doelman, J., Eitelberg, D. A., Engstrom, K., Fujimori, S., Hasegawa, T., Havlik, P., Humpenoder, F., Jain, A. K., Krisztin, T., Kyle, P., Meiyappan, P., Popp, A., Sands, R. D., Schaldach, R., Schungel, J., Stehfest, E., Tabeau, A., Van Meijl, H., Van Vliet, J., and Verburg, P. H.: Hotspots of uncertainty in land-use and land-cover change projections: a global-scale model comparison, Glob. Change Biol., 22, 3967–3983, https://doi.org/10.1111/gcb.13337, 2016.

Pugh, T. A. M., MacKenzie, A. R., Hewitt, C. N., Langford, B., Edwards, P. M., Furneaux, K. L., Heard, D. E., Hopkins, J. R., Jones, C. E., Karunaharan, A., Lee, J., Mills, G., Misztal, P., Moller, S., Monks, P. S., and Whalley, L. K.: Simulating atmospheric composition over a South-East Asian tropical rainforest: performance of a chemistry box model, Atmos. Chem. Phys., 10, 279–298, https://doi.org/10.5194/acp-10-279-2010, 2010.

Pugh, T. A. M., Arneth, A., Olin, S., Ahlström, A., Bayer, A. D., Klein Goldewijk, K., Lindeskog, M., and Schurgers, G.: Simulated carbon emissions from land use change are substantially enhanced by accounting for agricultural management, Environ. Res. Lett., 10, 124008, https://doi.org/10.1088/1748-9326/10/12/124008, 2015.

Pyle, J. A., Warwick, N. J., Harris, N. R. P., Abas, M. R., Archibald, A. T., Ashfold, M. J., Ashworth, K., Barkley, M. P., Carver, G. D., Chance, K., Dorsey, J. R., Fowler, D., Gonzi, S., Gostlow, B., Hewitt, C. N., Kurosu, T. P., Lee, J. D., Langford, S. B., Mills, G., Moller, S., MacKenzie, A. R., Manning, A. J., Misztal, P., Nadzir, M. S. M., Nemitz, E., Newton, H. M., O'Brien, L. M., Ong, S., Oram, D., Palmer, P. I., Peng, L. K., Phang, S. M., Pike, R., Pugh, T. A. M., Rahman, N. A., Robinson, A. D., Sentian, J., Abu Samah, A., Skiba, U., Ung, H. E., Yong, S. E., and Young, P. J.: The impact of local surface changes in Borneo on atmospheric composition at wider spatial scales: coastal processes, land-use change and air quality, Philos. T. R. Soc. B, 366, 3210–3224, https://doi.org/10.1098/rstb.2011.0060, 2011.

Reilly, J., Melillo, J., Cai, Y. X., Kicklighter, D., Gurgel, A., Paltsev, S., Cronin, T., Sokolov, A., and Schlosser, A.: Using Land To Mitigate Climate Change: Hitting the Target, Recognizing the Trade-offs, Environ. Sci. Technol., 46, 5672–5679, https://doi.org/10.1021/es2034729, 2012.

Reiner, D. M.: Learning through a portfolio of carbon capture and storage demonstration projects, Nat. Energy, 1, 15011, https://doi.org/10.1038/Nenergy.2015.11, 2016.

Rodriguez, J. P., Beard, T. D., Bennett, E. M., Cumming, G. S., Cork, S. J., Agard, J., Dobson, A. P., and Peterson, G. D.: Trade-offs across space, time, and ecosystem services, Ecol. Soc., 11, 28, https://doi.org/10.5751/ES-01667-110128, 2006.

Rogelj, J., Luderer, G., Pietzcker, R. C., Kriegler, E., Schaeffer, M., Krey, V., and Riahi, K.: Energy system transformations for limiting end-of-century warming to below 1.5 °C, Nat. Clim. Change, 5, 519–527, https://doi.org/10.1038/nclimate2572, 2015.

Rosenkranz, M., Pugh, T. A. M., Schnitzler, J. P., and Arneth, A.: Effect of land-use change and management on biogenic volatile organic compound emissions – selecting climate-smart cultivars, Plant Cell Environ., 38, 1896–1912, https://doi.org/10.1111/pce.12453, 2015.

Samir, K. C. and Lutz, W.: The human core of the shared socioeconomic pathways: Population scenarios by age, sex and level of education for all countries to 2100, Global Environ. Chang., 42, 181–192, https://doi.org/10.1016/j.gloenvcha.2014.06.004, 2017.

Sampaio, G., Nobre, C., Costa, M. H., Satyamurty, P., Soares, B. S., and Cardoso, M.: Regional climate change over eastern Amazonia caused by pasture and soybean cropland expansion, Geophys. Res. Lett., 34, L17709, https://doi.org/10.1029/2007gl030612, 2007.

Santangeli, A., Toivonen, T., Pouzols, F. M., Pogson, M., Hastings, A., Smith, P., and Moilanen, A.: Global change synergies and trade-offs between renewable energy and biodiversity, Gcb Bioenergy, 8, 941–951, https://doi.org/10.1111/gcbb.12299, 2016.

Schurgers, G., Arneth, A., Holzinger, R., and Goldstein, A. H.: Process-based modelling of biogenic monoterpene emissions combining production and release from storage, Atmos. Chem.

Phys., 9, 3409–3423, https://doi.org/10.5194/acp-9-3409-2009, 2009.

Scott, C. E., Rap, A., Spracklen, D. V., Forster, P. M., Carslaw, K. S., Mann, G. W., Pringle, K. J., Kivekäs, N., Kulmala, M., Lihavainen, H., and Tunved, P.: The direct and indirect radiative effects of biogenic secondary organic aerosol, Atmos. Chem. Phys., 14, 447–470, https://doi.org/10.5194/acp-14-447-2014, 2014.

Scott, V., Haszeldine, R. S., Tett, S. F. B., and Oschlies, A.: Fossil fuels in a trillion tonne world, Nat. Clim. Change, 5, 419–423, https://doi.org/10.1038/Nclimate2578, 2015.

Searle, S. Y. and Malins, C. J.: Will energy crop yields meet expectations?, Biomass Bioenerg., 65, 3–12, https://doi.org/10.1016/j.biombioe.2014.01.001, 2014.

Sillman, S.: The relation between ozone, NO_x and hydrocarbons in urban and polluted rural environments, Atmos. Environ., 33, 1821–1845, https://doi.org/10.1016/S1352-2310(98)00345-8, 1999.

Slade, R., Bauen, A., and Gross, R.: Global bioenergy resources, Nat. Clim. Change, 4, 99–105, https://doi.org/10.1038/Nclimate2097, 2014.

Smith, B., Wårlind, D., Arneth, A., Hickler, T., Leadley, P., Siltberg, J., and Zaehle, S.: Implications of incorporating N cycling and N limitations on primary production in an individual-based dynamic vegetation model, Biogeosciences, 11, 2027–2054, https://doi.org/10.5194/bg-11-2027-2014, 2014.

Smith, L. J. and Torn, M. S.: Ecological limits to terrestrial biological carbon dioxide removal, Climatic Change, 118, 89–103, https://doi.org/10.1007/s10584-012-0682-3, 2013.

Smith, P., Ashmore, M. R., Black, H. I. J., Burgess, P. J., Evans, C. D., Quine, T. A., Thomson, A. M., Hicks, K., and Orr, H. G.: The role of ecosystems and their management in regulating climate, and soil, water and air quality, J. Appl. Ecol., 50, 812–829, https://doi.org/10.1111/1365-2664.12016, 2013.

Smith, P., Davis, S. J., Creutzig, F., Fuss, S., Minx, J., Gabrielle, B., Kato, E., Jackson, R. B., Cowie, A., Kriegler, E., van Vuuren, D. P., Rogelj, J., Ciais, P., Milne, J., Canadell, J. G., McCollum, D., Peters, G., Andrew, R., Krey, V., Shrestha, G., Friedlingstein, P., Gasser, T., Grubler, A., Heidug, W. K., Jonas, M., Jones, C. D., Kraxner, F., Littleton, E., Lowe, J., Moreira, J. R., Nakicenovic, N., Obersteiner, M., Patwardhan, A., Rogner, M., Rubin, E., Sharifi, A., Torvanger, A., Yamagata, Y., Edmonds, J., and Cho, Y.: Biophysical and economic limits to negative CO_2 emissions, Nat. Clim. Change, 6, 42–50, https://doi.org/10.1038/Nclimate2870, 2016.

Stehfest, E., van Vuuren, D., Kram, T., Bouwman, L., Alkemade, R., Bakkenes, M., Biemans, H., Bouwman, A., den Elzen, M., Janse, J., Lucas, P., van Minnen, J., Müller, C., and Prins, A.: Integrated Assessment of Global Environmental Change with IMAGE 3.0: Model description and policy applications, The Hague, PBL Netherlands Environmental Assessment Agency, The Hague, the Netherlands, 2014.

Sterling, S. M., Ducharne, A., and Polcher, J.: The impact of global land-cover change on the terrestrial water cycle, Nat. Clim. Change, 3, 385–390, https://doi.org/10.1038/Nclimate1690, 2013.

Tilman, D., Cassman, K. G., Matson, P. A., Naylor, R., and Polasky, S.: Agricultural sustainability and intensive production practices,

Nature, 418, 671–677, https://doi.org/10.1038/nature01014, 2002.

Unger, N.: Human land-use-driven reduction of forest volatiles cools global climate, Nat. Clim. Change, 4, 907–910, https://doi.org/10.1038/nclimate2347, 2014.

Valin, H., Sands, R. D., van der Mensbrugghe, D., Nelson, G. C., Ahammad, H., Blanc, E., Bodirsky, B., Fujimori, S., Hasegawa, T., Havlik, P., Heyhoe, E., Kyle, P., Mason-D'Croz, D., Paltsev, S., Rolinski, S., Tabeau, A., van Meijl, H., von Lampe, M., and Willenbockel, D.: The future of food demand: understanding differences in global economic models, Agr. Econ.-Blackwell, 45, 51–67, https://doi.org/10.1111/agec.12089, 2014.

Val Martin, M., Heald, C. L., Lamarque, J.-F., Tilmes, S., Emmons, L. K., and Schichtel, B. A.: How emissions, climate, and land use change will impact mid-century air quality over the United States: a focus on effects at national parks, Atmos. Chem. Phys., 15, 2805–2823, https://doi.org/10.5194/acp-15-2805-2015, 2015.

van Dijk, A. I. J. M., van Noordwijk, M., CaldeR, I. R., Bruijnzeel, S. L. A., Schellekens, J., and Chappell, N. A.: Forest-flood relation still tenuous – comment on "Global evidence that deforestation amplifies flood risk and severity in the developing world" by Bradshaw et al., Glob. Change Biol., 15, 110–115, https://doi.org/10.1111/j.1365-2486.2008.01708.x, 2009.

van Vliet, J., Bregt, A. K., Brown, D. G., van Delden, H., Heckbert, S., and Verburg, P. H.: A review of current calibration and validation practices in land-change modeling, Environ. Modell. Softw., 82, 174–182, https://doi.org/10.1016/j.envsoft.2016.04.017, 2016.

van Vuuren, D. P., Edmonds, J., Kainuma, M., Riahi, K., Thomson, A., Hibbard, K., Hurtt, G. C., Kram, T., Krey, V., Lamarque, J. F., Masui, T., Meinshausen, M., Nakicenovic, N., Smith, S. J., and Rose, S. K.: The representative concentration pathways: an overview, Climatic Change, 109, 5–31, https://doi.org/10.1007/s10584-011-0148-z, 2011.

van Vuuren, D. P., Deetman, S., van Vliet, J., van den Berg, M., van Ruijven, B. J., and Koelbl, B.: The role of negative CO_2 emissions for reaching 2 °C-insights from integrated assessment modelling, Climatic Change, 118, 15–27, https://doi.org/10.1007/s10584-012-0680-5, 2013.

Viglizzo, E. F., Paruelo, J. M., Laterra, P., and Jobbagy, E. G.: Ecosystem service evaluation to support land-use policy, Agr. Ecosyst. Environ., 154, 78–84, https://doi.org/10.1016/j.agee.2011.07.007, 2012.

Visconti, P., Pressey, R. L., Giorgini, D., Maiorano, L., Bakkenes, M., Boitani, L., Alkemade, R., Falcucci, A., Chiozza, F., and Rondinini, C.: Future hotspots of terrestrial mammal loss, Philos. T. Roy. Soc. B, 366, 2693–2702, https://doi.org/10.1098/rstb.2011.0105, 2011.

Warszawski, L., Frieler, K., Huber, V., Piontek, F., Serdeczny, O., and Schewe, J.: The Inter-Sectoral Impact Model Intercomparison Project (ISI-MIP): Project framework, P. Natl. Acad. Sci. USA, 111, 3228–3232, https://doi.org/10.1073/pnas.1312330110, 2014.

Whitehead, P. G., Wilby, R. L., Battarbee, R. W., Kernan, M., and Wade, A. J.: A review of the potential impacts of climate change on surface water quality, Hydrolog. Sci. J., 54, 101–123, https://doi.org/10.1623/hysj.54.1.101, 2009.

Wilkinson, S., Mills, G., Illidge, R., and Davies, W. J.: How is ozone pollution reducing our food supply?, J. Exp. Bot., 63, 527–536, https://doi.org/10.1093/jxb/err317, 2012.

Williamson, P.: Scrutinize CO_2 removal methods, Nature, 530, 153–155, https://doi.org/10.1038/530153a, 2016.

Wiltshire, A. and Davies-Barnard, T.: Planetary limits to BECCS negative emissions, AVOID2 WPD.2a Report 1, available at: http://www.avoid.uk.net/2015/07/planetary-limits-to-beccs-negative-emissions-d2a/ (last access: 27 October 2017), 2015.